

**EFFECTS ON MICROWAVE SIGNAL  
PROPAGATION DUE TO LAYER BASED  
INTENSITY VARIATION OF SAND/DUST  
STORM**

BY

**MAHFUZ ULLAH**

A Thesis Presented to the  
DEANSHIP OF GRADUATE STUDIES

**KING FAHD UNIVERSITY OF PETROLEUM & MINERALS**

DHAHRAN, SAUDI ARABIA

In Partial Fulfillment of the  
Requirements for the Degree of

**MASTER OF SCIENCE**

In

**ELECTRICAL ENGINEERING**

DECEMBER 2015

KING FAHD UNIVERSITY OF PETROLEUM & MINERALS

DHAHRAN- 31261, SAUDI ARABIA

**DEANSHIP OF GRADUATE STUDIES**

This thesis, written by **MAHFUZ ULLAH** under the direction his thesis advisor and approved by his thesis committee, has been presented and accepted by the Dean of Graduate Studies, in partial fulfillment of the requirements for the degree of **MASTER OF SCIENCE IN ELECTRICAL ENGINEERING**.



Dr. Ali Ahmad Al-Shaikhi  
Department Chairman



Dr. Salam A. Zummo  
Dean of Graduate Studies



Dr. Sheikh Sharif Iqbal  
(Advisor)



Dr. Hussain Ali Jamid  
(Member)



Dr. Wajih A. Abu Al-Saud  
(Member)

3/2/16  
Date

*©Mahfuz Ullah*

*December, 2015*

|

*Dedicated to*  
*my beloved parents, MD. Motiur Rahman &*  
*Mrs. Denarajadi Begum*  
*and to my wife*  
*Nusaiba Binte Mahbub |*

## **ACKNOWLEDGMENTS**

All praises and worship belong to Allah, the most Beneficent, the most merciful. May the peace and blessing of Allah be upon the last Prophet Muhammad Sallallahu Alaihi Wa Sallam, his family, his companions, and all of his followers.

I am grateful to my family for being there with me all the time. It is their sacrifice and emotional support that helped me to get through my tough times. I deeply thank my parents, my wife, my brother, and my in laws for the selfless love they have showered on me. May Allah reward them the best in this world and in the hereafter.

I am deeply humbled and blessed to be supervised by Dr. Sheikh Sharif Iqbal. Throughout my thesis work, he has mentored me with his excellent skills, deep understanding on the subject matters and sharp vision. I am indebted to him for the patience, support, inspiration and encouragement he has provided me. His work ethic and dedication has taught me some invaluable lessons that I shall carry with me all my life.

I express my sincere appreciation to Dr. Hussain Ali Jamid (EE Dept. KFUPM) and Dr. Wajih Abu Al-Saud (EE Dept. KFUPM) to be the part of the thesis committee. Their valuable evaluations, advice and suggestions have brought major improvements to this thesis work for which I express my gratitude.

I also want to thank all my KFUPM graduate colleagues and friends who helped me through various means. I wish to thank Imran Reza and Tri Bagus Susilo for their exceptional support, company and kindness. I appreciate the help of Samer, Jibril, Hesham, Saleh, Abdullah and Maan. I also express my gratitude towards ShafiUllah,

Kabir, Russel, Sujon, Shoaib, Fahmi, Modhu, Lipiar and all the members of Bangladeshi community at KFUPM for their support and affection.

# TABLE OF CONTENTS

<b>ACKNOWLEDGMENTS.....</b>	<b>V</b>
<b>TABLE OF CONTENTS.....</b>	<b>VII</b>
<b>LIST OF TABLES.....</b>	<b>XI</b>
<b>LIST OF FIGURES.....</b>	<b>XII</b>
<b>LIST OF ABBREVIATIONS.....</b>	<b>XVI</b>
<b>ABSTRACT.....</b>	<b>XVII</b>
<b>ABSTRACT IN ARABIC.....</b>	<b>XIX</b>
<b>CHAPTER 1 INTRODUCTION.....</b>	<b>1</b>
<b>1.1 Introduction.....</b>	<b>1</b>
<b>1.2 Thesis Objectives.....</b>	<b>7</b>
<b>1.3 Thesis Organization.....</b>	<b>8</b>
<b>CHAPTER 2 LITERATURE REVIEW.....</b>	<b>10</b>
<b>2.1 Attenuation Due To Sand-Dust Media.....</b>	<b>10</b>
<b>2.1.1 Attenuation Prediction Models.....</b>	<b>12</b>
<b>2.2 Dielectric Properties of Sand-Dust Media.....</b>	<b>14</b>

2.2.1	Permittivity and Loss Tangents.....	14
2.2.2	Particle Size and Distribution of Sand-Dust Media.....	15
<b>CHAPTER 3 ELECTROMAGNETIC PROPERTIES OF SAND/DUST MEDIUM.....</b>		<b>17</b>
3.1	Properties of Electromagnetic Waves.....	17
3.1.1	Maxwell’s Equations for a Lossy Dielectric Medium.....	18
3.1.2	Scattering Parameters (S-Parameters) .....	20
3.1.3	Guided Wave Propagation through Dielectric Media.....	21
3.1.4	Different Modes for Propagation.....	22
3.2	Dielectric Properties of Sand.....	24
3.2.1	Permittivity.....	24
3.2.2	Dielectric Loss Tangent.....	24
3.3	Soil Taxonomy.....	25
3.4	High Frequency Structural Simulator (HFSS) .....	27
<b>CHAPTER 4 EXPERIMENTAL VERIFICATION OF THE SIMULATION MODEL OF SANDY/DUSTY MEDIA .....</b>		<b>31</b>
4.1	Propagation Through Guided Media.....	31
4.1.1	Propagation Modes.....	32
4.1.2	Horn Antenna.....	33



4.1.3	Sieve Analysis to Separate Sand/Dust Samples.....	35
4.1.4	Experimental Set-up for Propagation through Rectangular W/G.....	38
4.1.5	Experimental Results for Waveguide Excited by Coaxial Feed.....	39
4.1.6	Experimental Results for Waveguide Excited by Horn Antenna.....	40
4.1.7	Simulated Results for Guided Propagation Using HFSS.....	43
4.2	Propagation through Non-Guided Media.....	45
4.2.1	Experimental Results for Non-Guided Propagation.....	49
4.2.2	Simulated Results for Non-Guided Propagation.....	51
 <b>CHAPTER 5 SIMULATOR BASED ANALYSIS OF MW PROPAGATION THROUGH SANDY/DUSTY MEDIA.....</b>		<b>55</b>
5.1	Background of the Modified Simulation Model.....	55
5.2	Modified Simulation Model with Sand/Dust Samples.....	58
5.2.1	Investigated Parameters of the Sand/Dust Media.....	60
5.3	Investigation for Spherical Shaped Sand Particles.....	60
5.3.1	For Different Size of Sand Particles.....	60
5.3.2	For Different Concentration of Sand Particles.....	64
5.4	Investigation for Elliptical Shaped Sand Particles.....	68
5.4.1	For Different Size of Sand Particles .....	68
5.4.2	For Different Concentration of Sand Particles .....	72

<b>CHAPTER 6 COMPARISON OF SIMULATION AND EXPERIMENTAL RESULTS</b>	<b>76</b>
6.1 Relating Simulation Results to Experimental Observations.....	76
6.1.1 Design and Analysis of Scaled Simulated Model.....	77
6.1.2 Comparison of Attenuation With Values Obtained from Literature.....	82
6.2 Investigation of Effects of Polarization Through Simulation .....	83
<b>CHAPTER 7 SUMMARY AND CONCLUSION.....</b>	<b>86</b>
7.1 Summary.....	86
7.2 Conclusion.....	89
7.3 Future Works.....	90
<b>REFERENCES.....</b>	<b>91</b>
<b>VITAE.....</b>	<b>97</b>

## LIST OF TABLES

Table 3.1	Dielectric constants for different types of soil/sand.....	27
Table 4.1	The cut off frequencies (GHz) of rectangular waveguide.....	33
Table 4.2	Experimental results for guided propagation excited by coaxial probe.....	40
Table 4.3	Experimental results for guided propagation excited by horn antenna.....	42
Table 4.4	Simulated S parameters for rectangular waveguide.....	45
Table 6.1	Simulated and Experimental $S_{21}$ responses with their corresponding losses.....	81
Table 6.2	Attenuation due to sand particles for an 80 cm link.....	81
Table 6.3	Comparison of the different Attenuation values (dB/m).....	83
Table 6.4	Simulated $S_{21}$ values for different polarizations and different shapes of sand particles.....	84

## LIST OF FIGURES

Figure 1.1	Sand Storm observed in a KFUPM play ground, during (above) and after (below) the storm, April, 2014.....	2
Figure 1.2	A huge cloud of sand covers a coastal area in Australia, 2013 [2].....	3
Figure 2.1	A summary of the literature review.....	16
Figure 3.1	A linearly polarized Electromagnetic Wave.....	18
Figure 3.2	A simple two port network.....	20
Figure 3.3	Rectangular Waveguide.....	22
Figure 3.4	Field patterns of some dominant modes for waveguides.....	23
Figure 3.5	Soil texture in triangular format [31].....	25
Figure 3.6	Map of soil grain sizes and types in the Middle East [32].....	26
Figure 3.7	Simulated model of the rectangular waveguide in HFSS.....	28
Figure 3.8	Wave port in construction for simulating S parameter responses for the waveguide.....	29
Figure 3.9	Material selection in HFSS simulation software.....	29
Figure 3.10	Window for choosing frequency sweep.....	30
Figure 4.1	Schematic diagram of a rectangular waveguide.....	31
Figure 4.2	Photograph of the set up that was used for guided measurements.....	32
Figure 4.3	Schematic diagram of a Horn Antenna.....	34

Figure 4.4	Photograph of the Horn Antenna used to excite the waveguide.....	34
Figure 4.5	The mechanical shaker used for Sieve Analysis.....	36
Figure 4.6	Loading sand samples in the Sieve analysis setup.....	36
Figure 4.7	Separation of sand samples through mechanical shaking.....	37
Figure 4.8	Separated sand samples of diameter 90 $\mu\text{m}$ , 125 $\mu\text{m}$ , and 150 $\mu\text{m}$ .....	37
Figure 4.9	Inducing Sand storm within the rectangular waveguide.....	39
Figure 4.10	Measurement of S-parameters for guided propagation with 90 $\mu\text{m}$ sand samples.....	41
Figure 4.11	Measurement of S-parameters for guided propagation with 125 $\mu\text{m}$ sand samples.....	41
Figure 4.12	Measurement of S-parameters for guided propagation with 150 $\mu\text{m}$ sand samples.....	42
Figure 4.13	Air-sand/air-dust filled waveguide, excited by ideal port.....	44
Figure 4.14	Plastic Box built for investigation of non guided propagation.....	46
Figure 4.15	Schematic diagram for non-guided attenuation measurement setup.....	47
Figure 4.16	Non-guided attenuation measurement setup with loaded sand samples of 300 gm.....	47
Figure 4.17	Propagation through air-sand media with concentration of 1.04 $\text{kg/m}^3$ ..	48
Figure 4.18	Comparison of measured attenuation of MW signal at 9 GHz, propagating through three sand samples.....	50
Figure 4.19	Simulator model of air-sand or air-dust filled box excited by horn antenna.....	51

Figure 4.20	Comparing attenuation for different $\epsilon_{\text{eff}}$ , for non guided propagation.....	52
Figure 4.21	Comparing simulation of $\epsilon_{\text{eff}}=2$ with the experimental results using $90 \mu\text{m}$ particles.....	53
Figure 4.22	Comparing simulation of $\epsilon_{\text{eff}}=2.7$ with the experimental results using $125 \mu\text{m}$ particles.....	53
Figure 4.23	Comparing simulation of $\epsilon_{\text{eff}}=3$ with the experimental results using $150 \mu\text{m}$ particles.....	54
Figure 5.1	Simulated propagation box between a pair of horn antennas.....	57
Figure 5.2	Simulator model with 105 circular, $\epsilon_{\text{eff}}=3$ and randomly distributed sand-dust samples, for particle radius of 0.10 cm.....	58
Figure 5.3	The magnitude response of S21 and S11 for 105 spherical shaped sand particles.....	59
Figure 5.4	The phase response of S21 and S11 for 105 spherical shaped sand particles .....	59
Figure 5.5	S21 response for sand concentration of 63 spherical particles/unit-box.	61
Figure 5.6	S21 response for sand concentration of 105 spherical particles /unit-box.....	62
Figure 5.7	S21 response for sand concentration of 135 spherical particles /unit-box.....	63
Figure 5.8	S21 response for spherical sand radius of 0.05 cm.....	65
Figure 5.9	S21 response for spherical sand radius of 0.10 cm.....	65
Figure 5.10	S21 response for spherical sand radius of 0.25 cm.....	66

Figure 5.11	S21 response for spherical sand radius of 0.38 cm.....	66
Figure 5.12	Comparison of S21 measurements for variation in sand concentration..	67
Figure 5.13	A tri-axial ellipsoid.....	68
Figure 5.14	S21 response for sand concentration of 135 vertically oriented elliptic sand particles.....	70
Figure 5.15	S21 response for sand concentration of 135 horizontally oriented elliptic sand particles.....	71
Figure 5.16	Comparison for elliptical shaped sand particles with spherical shaped sand particles, for fixed concentration of 135 sand particles.....	72
Figure 5.17	S21 responses for elliptical sand particle with $a=b=0.25$ cm, $c=0.2$ cm (vertical orientation).....	73
Figure 5.18	S21 responses for elliptical sand particle with $a=b=0.25$ cm, $c=0.2$ cm (horizontal orientation).....	74
Figure 5.19	Comparison for elliptical shaped particles ( $a=b=0.25$ cm, $c=0.2$ cm) with spherical shaped sand particles ( $r=0.25$ cm).....	75
Figure 6.1	Simulated responses for Box A at 1.5 GHz are equivalent to the experimental responses for Box B at 9 GHz.....	79
Figure 6.2	Comparison of simulated $S_{21}$ responses of Air-Sand mixture and Air-only cases Box A.....	80

## **LIST OF ABBREVIATIONS**

EM	Electro Magnetic
HFSS	High Frequency Structural Simulator
KFUPM	King Fahd University of Petroleum and Minerals
MW	Micro Wave
QoS	Quality of Service
RF	Radio Frequency
S parameters	Scattering Parameters
TE	Transverse Electric
TM	Transverse Magnetic
USDA	United States Department of Agriculture
W/G	Waveguide



## ABSTRACT

Full Name : [Mahfuz Ullah]  
Thesis Title : [Effects On Microwave Signal Propagation Due To Layer Based Intensity Variation of Sand/Dust Storm]  
Major Field : [Electrical Engineering]  
Date of Degree : [December, 2015]

[In Saudi Arabia, severe sand/dust storms can limit the quality of service (QoS) for broadband communication channels. Thus, modeling of Microwave attenuation in different height of sand/dust storms is essential to optimize the link budget of communication channels. Although several models exist to predict the electromagnetic (EM) scattering in sand-dust storms, they are mostly dependent on visibility measurements at the epicenter of the storm. In addition to this inconvenient task, these models do not include multiple scattering effects from suspended sand and dust particles. In this research work, guided and non-guided experimental methods are used to investigate the degradation of Microwave signal propagating through an air-sand and air-dust media. The process is started by collecting multiple dust/sand (with diameter of particles =90  $\mu\text{m}$ , 125  $\mu\text{m}$ , and 150  $\mu\text{m}$ ) samples through sieve analysis. A test box is fabricated with an air valve that allows the flow of pressurized air with negligible sand-dust leakage. This process is used to create a sand or dust storm like media within the box. Horn antennas that are optimally integrated on both ends, measure the magnitude and phase of the S-parameter responses. The measured responses ( $S_{21}$ ) are used to validate a simulated model of a similar setup. The software model is used to analyze the influence of sand-dust media parameters, such as particle-size, shape, concentration,

polarization and effective permittivity, on the propagating X-band signal. The analyzed data show that the model could be proven useful in predicting signal attenuation considering the effects of different parameters related to Sandy/Dusty weather. Finally the simulated results are linked to the experimentally observed measurements by calculating attenuation due to presence of sand for a 1 m link and compared with values obtained from literature.

## ملخص الرسالة

الاسم الكامل: محفوظ الله

عنوان الرسالة: تأثير التغيرات الطبقيه للعواصف الغباريه او الرملية على انتشار امواج الميكرويف

التخصص: الهندسة الكهربائية

تاريخ الدرجة العلمية: كانون اول, 2015

في المملكة العربية السعودية، يمكن لعديد من العواصف الرملية والغبارية ان تؤثر على جودة خدمة قنوات الاتصال واسع النطاق. ولهذا، تم وضع نموذج لتقدير التدهور في اشارة الميكرويف في حالات العواصف الرملية والغبارية القوية من اجل تحسين وتطوير ميزانية الربط عبر هذه القنوات. وعلى الرغم من وجود العديد من النماذج المختلفة لتقدير النثر الكهرومغناطيسي (EM) الناتج من هذه العواصف، لكنها تعتمد على قياسات واضحة الرؤية من بؤرة العاصفة!. اضافة الى هذا المتطلب غير المريح، فإن هذه النماذج لا تحتوي وصف التأثيرات المتعددة على النثر الناتج من جسيمات ودقائق الرمال والغبار في هذه العواصف.

في هذا العمل البحثي تم استخدام طرق تجريبية موجهة وغير موجهة من اجل التحقق من كمية ندهور اشارة الميكرويف عند الانتشار في الوسط الجوي خلال العواصف الرملية والغبارية. حيث بدأت هذه العملية عن طريق جمع عينات من الغبار والرمل باقطار جزيئية مختلفة بواسطة غربال تحليلي وهذه الاقطار كما يلي 90 ميكرومتر، و125 ميكرومتر، و 150 ميكرومتر. ثم تم تصميم صندوق اختبري مع صمام يسمح بتفق الهواء المضغوط وتسرب قليل من الرمال والغبار. حيث تم تركيب هوائيان من نوع Horn على الاطراف بطريقة مثالية تسمح بقياس مقدار وطور متغيرات معامل (S).

ان قراءات (S21) التي تم الحصول عليها تم استخدامها في التحقق من اداء النموذج عبر المحاكاة تحت نفس الاعدادات، ثم تم استخدام النموذج البرمجي من اجل تحليل اثر متغيرات وسط العاصفة كحجم جزيئات الرمال والغبار، وشكلها، وتركزها، وقطبيتها، ومقدار سماحيته الفعالة على انتشار الامواج من نوع نطاق (X).

تشير البيانات المحللة الى ان النموذج الموضوع كان ناجحا واثبت فعاليته في التنبؤ بمقدار التدهور الحاصل على الاشارة تحت تأثير عوامل مختلفة تتعلق باجواء العواصف الرملية والغبار. ثم في النهاية تم مقارنة هذه البيانات المقاسة بعد عملية المحاكاة مع بيانات موجوده ناتجه عن ابحاث لنماذج سابقه في هذا المجال.

# CHAPTER 1

## INTRODUCTION

### 1.1 Introduction

Quality of service (QoS) in different wireless communication channels is independent on natural phenomena like rain, dust-sand storm, and snow. The suspended particles of water, dust, or snow can cause attenuation, scattering, and cross polarization for the propagating signal, which may introduce communication errors. So it is imperative to take account of these features and study their effects on the signal propagation. In recent years, researchers have investigated these phenomena [1-10] but they are mostly based on experimentally collected data. Since in the gulf region, dust-sand storms often limit the performance of communication channels, the main goal of this research work is to develop a software model (experimentally verified) to predict microwave signal attenuation and scattering due to multi-layered dust-sand storm.

A sand and/or dust storm is a meteorological phenomenon. These are quite common in arid and semi arid regions, as shown in Figure 1.1 and in Figure 1.2. Figure 1.1 show two pictures of a playground inside the campus of King Fahd University of Petroleum and Minerals, the first one showing the ground during a sand storm and the second one shows the same playground after the storm. Storms like these arise when loose sand particles are moved from a dry surface by some strong wind and transported to some other place. In

many regions of the world, namely the Middle East, Africa, China, Australia, and some parts of South America, these storms are quite common and can affect large areas. The average duration of these storms is 2-3 hours, but sometimes they could last from few hours to several days [1]. A recent sand-dust storm in Australia is shown Figure 2. The reliability and stability of the communication links in these affected regions become a matter of concern in terms of Quality of Service.



Figure 1.1: Sand Storm observed in a KFUPM play ground, during (above) and after (below) the storm, April, 2014.



Figure 1.2: A huge cloud of sand covers a coastal area in Australia, 2013 [2].

Basic differences between sand and dust are often made by comparing the sizes of particles found in these media, which may have radii between  $0.5 \mu\text{m}$  to  $200 \mu\text{m}$ . Particles with radii larger than  $60 \mu\text{m}$  are called sand particles and those with radii less than  $60 \mu\text{m}$  are known as dust [3]. In some literatures this distinctive value of the radius is  $80 \mu\text{m}$  [4]. A pure sand storm is basically a thick layer of sand cloud. The majority of the terrestrial radio relays or satellite links are affected very little by the sand storms, because sand particles generally don't rise above 2 meters from the ground. But above

this height, there remains dust storm which comprises of smaller particles than sand and can reach to a height of several thousand feet [3], [5]. A calculation of attenuation is of significant concern for the latter type of storm. Visibility is an indicator of the concentration of the storm and to be considered as a dust storm, the visibility has to be less than 1 km. Visibility of less than 500 meter is known as ‘severe dust storm’ [4]. Moreover, in the tropical regions where humidity is quite high, presence of a certain amount of moisture content in the particles also affect wave propagation.

The attenuation and cross polarization of the microwave and millimeter wave signal due to the sand particles are of great importance. This attenuation is mostly caused due to two physical mechanisms:(i) absorption and (ii) scattering of energy by the suspended sand or/and dust particles. In addition, a sandy/dusty medium also introduces insertion phase shift in the propagating microwave signal, which can severely degrade the channel QoS, especially at the Ku-band [6]. In the literature, Rayleigh scattering approximation and Mie scattering theory are mostly used to model attenuation and cross polarization of microwave signal propagating through sandy-dusty media. Especially Rayleigh scattering approximation is used for particles that are smaller than the wavelength of the propagating wave. Mie scattering theory is considered in the cases of scattering and absorption of spherically shaped particles. However,most of the papers available in the literature use these theories to approximate scattering and absorption from uniform sand-dust media; excluding the possibility that electrical properties of the media may be different at different heights of the sand-dust storm [6], [7].

Electrical and geometrical properties of a sand-dust media those mostly affect the propagating microwave signal include dielectric constants( $\epsilon_r$ ), sand-dust particle sizes and their concentration. Although dielectric constant and particle sizes can be approximated from the literature, the concentration or distributions of the particles within the sand-dust storms are uncertain. Mostly the sand and dust particles are randomly distributed and oriented depending on the speed and direction of the wind. Furthermore, the geometries or shapes of the particles are classified as ellipsoids, cubes, spheres, etc. So finding a reasonable effective dielectric constant( $\epsilon_{\text{reff}}$ )is challenging, but critical in determining the electrical effects of sandy-dusty media. In the literature, this complex parameter is calculated as a function of sand and dust composition and measured visibility [8].For the calculation of signal attenuation, several models have been tried by several authors [9], [10], [13]. Despite the uncertainties of the parameters mentioned above, some models suggest that useful analysis and prediction can be done without having precise data for these uncertain parameters. Optical visibility and frequency of the propagating signal are the key parameters in these models, that include the works of Dong et al.[11], Goldhirsh [4], Ahmed et al.[12], Ahmed [13]. In other references it is specified that visibility is a measure to quantify sand concentration and can be used to predict signal attenuation in different sandy-dusty media[3], [6], [8], [12], [13]. Visibility measurements can also determine sand-dust particle sizes, as the intensity of received light increases with less dense sand-dust concentration. This leads to the concept of layered distribution of sand-dust through-out the sand-storm. Elsheikhet al. integrated this concept in their work by assuming uniform distribution of sand particles with an adjustment factor that accountsfor the vertical intensity variation of the sand-dust



storm[12]. Harb [7] proposed an attenuation model where vertical intensity variation of the visibility is used to predict attenuation. But unfortunately these models with layered uniform distribution of sand-dust particles are not experimentally verified.

In this research work, a simple microwave scattering technique shall be used to experimentally validate the proposed software model, which is capable of determining the electrical properties of layered sand-dust media. An investigation shall also be conducted to observe the nature of the propagating microwave signals due to changes in particle sizes and sand concentrations.

## 1.2 Thesis Objectives

The objectives and motivation of this work can be summarized as

- To conduct a thorough literature survey on microwave propagation through sandy and dusty media, resembling sand-storms.
- Collect local sand-dust samples and perform Sieve test to separate sand/dust samples of different particle size, i.e. diameter of 90 $\mu\text{m}$ , 125 $\mu\text{m}$  and 150 $\mu\text{m}$ .
- To assemble a microwave measurement setup to experimentally observe the propagation of the X-band microwave signal under sandy/dusty media with known particle size and concentration.
- Develop equivalent simulator-model using HFSS software. Compare the simulated results with experimental findings to fine tune the simulator model.
- Compare the simulated results with experimental finding to fine tune the software model.
- Using the simulator model, investigate how the attenuation and polarization of propagating microwave signal is affected by the parameters of the sand/dust particles, such as, particle size, shapes and concentrations. This allows the prediction of losses due to different layers of the sand storm.
- Compare the observed attenuation due to sand-dust particles with available attenuation/meter values from the literature.

### **1.3 Thesis Organization**

The remainder of the thesis is organized as the following

#### Chapter 1: Introduction

The first chapter introduces the concept of microwave signal propagation through sand/dust media. A brief discussion on the basic parameters which influences the propagation of signal is presented. The objectives of the thesis work and organization of the book are also given in this chapter.

#### Chapter 2: Literature Review

In the gulf region, sand-storms limit the performance of the wireless communication channels. This chapter summarizes the recent research work that investigates the EM wave propagation through sandy-dusty media.

#### Chapter 3: Electromagnetic Properties of Sand/Dust Media

This chapter briefly discusses common parameters used to investigate the interaction between the sandy-dusty media and the propagating microwave signal. These parameters include Maxwell's equations, scattering parameters, attenuation constant, different modes for propagation, dielectric properties of sand like permittivity, loss tangents etc.

#### Chapter 4: Experimental Verification of Simulation Model of Sandy/Dusty Medium

As a proof of principle, a simple non-guided microwave lab setup will be developed and discussed in this chapter. Sieve analysis will be used to separate sand samples with

different particle size and blowers will be used to create lab based sand storms. Microwave scattering technique and network analyzer will be used to monitor attenuation and reflection effects.

#### Chapter 5: Simulator Based Analysis of MW propagation through Sandy-Dusty Media

In this chapter, a professional software (HFSS) will be used to simulate the sand storm. The simulation responses will be compared with the experimental results. This process is essential to validate the simulation model, before using it to analyze EM propagation through multi layered dust media. For this analysis, two types of particle shapes shall be investigated. They are spherical and elliptical shaped sand particles.

#### Chapter 6: Comparison of Simulation and Experimental Results

This chapter shall try to relate the simulation model that was used in chapter 5 to the experimentally obtained measurements which is shown in chapter 4, through an extrapolation method. Finally polarization effects shall be observed for a particular simulation scenario.

#### Chapter 7: Conclusion and Future-work

In this chapter, the summary of the results and observations that are made during the research work will be discussed. Finally future research work that may add to these research findings will be mentioned.]

## **CHAPTER 2**

### **LITERATURE REVIEW**

Electromagnetic wave propagation through sand/dust storms is a widely researched area and several literatures are available to predict the attenuation and scattering of a microwave link. Some of these literatures are based on direct approaches, where real time data is collected and used to come up with theoretical models. Other literatures are based on an indirect approach, where calculations are based on the particle shapes/sizes and the dielectric constants etc. In this chapter, the available literatures are categorized on how the propagation properties of EM waves (attenuation/scattering/polarization) are affected by the electrical (dielectric constant) and physical (particle shape/size/density) properties of the sandy-dusty media. The categories are divided in terms of (a) Effects on Attenuation, (b) Dielectric Constants and Loss Tangent and (c) Particle Size and Distribution.

#### **2.1 Attenuation Due To Sand-Dust Media**

Al-Hafid et al. [15] summarized their observation of some real time data on propagation of microwave link. They took measurements for a 13 GHz communication link near the city of Baghdad, where it was found that the fade-depths to the received signals fall by 10 to 15 dB for tens of minutes at a time. These experimental results showed a much larger

attenuation than a predicted response, especially considering the very low dust concentration with visibility range of around 6-10 km.

J.W. Ryde [16] investigated the radar reflectivity of dust storms, which were negligible at frequencies lower than 30 GHz. Ahmad [17] investigated a communication link operating at 10 GHz and predicted that attenuation in clay (0.4 dB/km) is larger than that of sand (0.1 dB/km). In his calculations, he considered an upper limit of sand mass density to be  $10^{-5}$  g/cm<sup>3</sup>. In a similar research work, Ghobrial [20] predicted that the worst case of attenuation caused by a sandy-dusty media to an X-band EM wave is about  $10^{-3}$  dB/km. Here he assumed dielectric constant of the media as  $3.7 + j1.0$  with a dust density of  $10^6$  particles/m<sup>3</sup>. Ghobrial also investigated the attenuation of the propagating EM wave to the visibility related to the propagating media. For a visibility of 15 m, he predicted an attenuation of 0.25 dB/km for a propagating 14 GHz signal and an attenuation of 1.35 dB/km for a 37 GHz signal.

Chu [5] also proposed a relationship between visibilities with attenuation for microwave signal propagating through sandy/dusty media. He used the Rayleigh approximation and according to his findings: for a sandy-dusty medium with dielectric constant of  $10 + j1.0$ , suspending particle radius of 100  $\mu$ m and visibility of 0.15 km, the point attenuation is about 0.1 dB/km. In 1982, Ansari et al. [1] investigated the attenuation of EM waves through sandy-dusty media up to a frequency range of 37 GHz. Similar to Chu's work Haddad et al. [21] related attenuation to visibility. In this research work, dust storms were simulated inside a laboratory chamber and the findings indicated a much larger attenuation than the predicted results. The measured attenuation was 0.034 dB/m, whereas the calculated value was 0.001 dB/m, for a density of  $6 \times 10^{-5}$  g/cm<sup>3</sup> [21].

Rafuses'[22]research work on this topic concluded that EM signal attenuations due to sand and dust storm are negligible up to 44 GHz. For a 44 GHz signal, propagating through a storm with visibility of 100-200m, he predicted an attenuation of 0.085 to 0.2 dB/km, respectively.

### 2.1.1 Attenuation Prediction Model

Different theoretical models exist in the literature to calculate the attenuation of the electromagnetic wave propagating through sand-dust storms. Most of these models are heavily reliant on parameters like visibility (i.e. sand/dust concentration) and particle size of the sand/dust.

a. Work of Goldhirsh[4]:

Goldhirsh derived a formula of EM wave attenuation due to sandy-dusty media, based on the Rayleigh approximation. The formula is given in terms of frequency and visibility as,

$$\alpha = \frac{(2.317)(10^{-3})f}{V_b^\gamma \cdot \lambda} \left( \frac{\epsilon''}{(\epsilon' + 2)^2 + \epsilon''^2} \right) \left[ \frac{\text{dB}}{\text{m}} \right] \quad (1)$$

Here  $\lambda$  is wavelength in meter,  $\epsilon_m^* = \epsilon' - j\epsilon''$  is the dielectric constant of the dust particle,  $\gamma$  is a constant whose value is chosen to be 1.07,  $V_b$  is the visibility in kilometers and 'f' is the frequency of the EM wave link in GHz.

b. Work of Ahmed et al. [12]:

Ahmed et al. also derived similar attenuation model as a function of visibility. His formula was based on Mie scattering theory and measured probability density function and can be expressed as:

$$\alpha = \frac{5.67 \times r_e}{V_b \times \lambda} \left( \frac{\epsilon''}{(\epsilon' + 2)^2 + \epsilon''^2} \right) \left[ \frac{\text{dB}}{\text{m}} \right] \quad (2)$$

Here  $\epsilon_m^* = \epsilon' - j\epsilon''$  is the dielectric constant of the dust particle and  $r_e$  is the effective particle radius of sand inside the propagation medium. It is considered as third to second moment of size distribution of the sand particles and expressed as  $\frac{\sum_i p_i r_i^3}{\sum_i p_i r_i^2}$ .  $p_i$  is the probability associated with the particle radius  $r_i$ .

c. Work of Donget al. [11]:

The attenuation formula derived by Dong et al. was expressed in terms of frequency and visibility as;

$$\alpha = \frac{(2.573)(10^{-3}) f}{V_b^\gamma} \text{Im} \left( \frac{\epsilon_m^* - 1}{\epsilon_m^* + 2} \right) \left[ \frac{\text{dB}}{\text{m}} \right] \quad (3)$$

Here too, the value of the constant  $\gamma$  is chosen as 1.07.

d. Work of Ahmed [13]:

Ahmed derived [13] another attenuation formula based on Rayleigh approximation and given by

$$\alpha = \frac{0.629 \times 10^3 f r_e}{V_b} \left( \frac{\epsilon''}{(\epsilon' + 2)^2 + \epsilon''^2} \right) \left[ \frac{\text{dB}}{\text{m}} \right] \quad (4)$$

Here,  $r_e$  is the effective particle radius of sand.



Note that all the above models for predicting EM wave attenuation require measuring visibility, which is often difficult and dangerous at the epicentre of the dust/sand storm. So this thesis proposes an alternative microwave model to predict attenuation, which requires knowledge about the electrical parameters of media (dielectric constant of the media, wave polarization etc).

## **2.2 Dielectric Properties of Sand-Dust Media**

### **2.2.1 Permittivity and Loss Tangents**

Uncertainty about the complex dielectric constants ( $\epsilon_m$ ) has been a subject of extensive study for quite some time [18] [19]. Ahmed [17] made a series of measurements at 10 GHz and found that sand permittivity as  $3.8 + j0.038$  by extrapolating to the  $\epsilon$  vs density plot of solid material. He also tried to find some mean permittivities of some compressed samples by packing them into a short circuited waveguide and making reflection measurements. Later Al Baderet al. [23] also measured permittivity by putting the samples inside waveguide. For 10 GHz they calculated  $\epsilon$  as  $2.5 + j0.072$ . Al Hafidet al. [15] also made measurements of sand-dust particles permittivity using an open resonator and the measured loss tangent was very low (0.00024). Chu [5] made assumptions regarding permittivity of spherical sand-dust particles with radius ranging from 0.01 to 0.1 mm and found the range of  $\epsilon$  from  $2.5 + j0.025$  to  $10 + j0.1$  for dry-soil to desert-sands, respectively. In the findings of Ghobrial [24], dielectric loss (loss tangent) for the sand-dust particles were observed to increase by 0.03 for a 4.3% increase in the moisture

contents within the sample. These results are larger compared to the loss-tangent approximated in Chu's work (i.e. 0.01). Sharif et al. [25] made measurements on the effect of moisture contents and chemical composition on dust permittivity. The mean  $\epsilon$  for several samples of dehydrated soil was measured as  $5.23 + j0.26$ . In the research work of Al-Bader et al. [23], the loss tangent was observed to decrease with particle size. This was expected as  $\epsilon_{\text{eff}}$  also decreases to some extent with particle size.

### **2.2.2 Particle Size and Distribution of Sand-Dust Media**

Ryde [16] first made a distinction between sand and dust storm. He said particles greater than 75 microns are considered sand and they can rise at most at a height of 2 m. In his investigation, a thick sand-dust surface layer of 1 cm was raised to a height of 300 m and the suspended sand-dust density was found to be  $7 \times 10^{-5} \text{ g/cm}^3$ . Ghobrialet al. [20] considered a suspended dust density of  $10^6$  particles per  $\text{m}^3$ . During the measured particle size distribution in the city of Khartoum, a maximum radius of dust particle was found to be 150 microns. In a similar observation Al-Bader et al. [23] also concluded that the maximum particle radius for an air borne sample of dust (also called as 'mainly clay') is 150 microns. Goldhirsh [26] showed that in a sand storm, suspended sand-dust density of  $10^8$  particles per  $\text{m}^3$  corresponds to a visibility of 4 to 5 meters. In another observation, Ghobrial[29] reported that the mean diameter of dust particles is less than  $50 \mu\text{m}$ . This estimation was based on measurements performed on four different Sand and Dust storms. Ansari et al. [1] reported that the particle distribution is exponential and most particles had a maximum radius of  $150 \mu\text{m}$ . According to the work of Sharif [30], particles may have an average diameter of  $134 \mu\text{m}$ .

In the literature, most commonly used particle size distributions includes Gaussian distribution (normal), log-normal distribution and Rosin-Rammler distribution. Ahmed [13] analyzed 16 samples of five different sand-dust storm in Riyadh and concluded that 14 of them can be considered of log-normal distribution and the remaining two can be specified by the power law. He used the square method of fitting in these observations.

An overall view on the literature review which is done for this work is presented below in Figure 2.1.

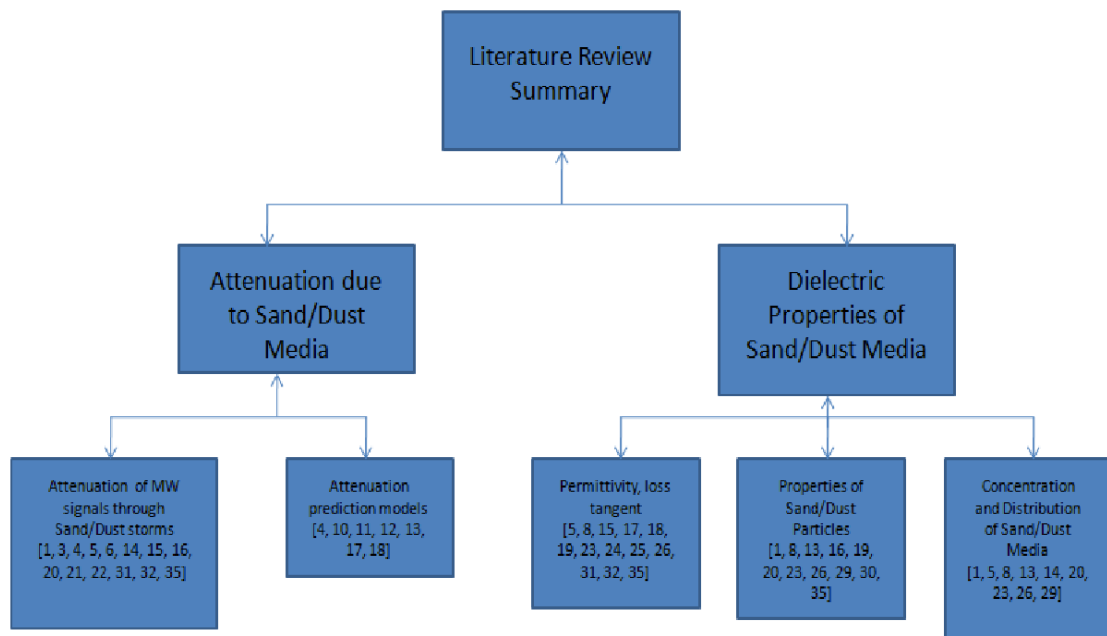


Figure 2.1: A summary of the literature review

## CHAPTER 3

# ELECTROMAGNETIC PROPERTIES OF SAND/DUST MEDIUM

### 3.1 Properties of Electromagnetic Waves

Electromagnetic (EM) waves can travel through a media or through free space (vacuum), whereas mechanical waves require a medium in order to travel from one position to another. An electromagnetic wave consists of oscillating orthogonal electric and magnetic fields components in directions perpendicular to the propagating EM wave. Frequency spectrum of EM wave is divided into different frequency bands based on their application [30].

Some basic properties of Electromagnetic waves can be summarized as;

1. In vacuum/air, EM waves travel at a constant speed of  $3 \times 10^8 \text{ ms}^{-1}$ .
2. The EM waves are transverse in nature as the E and H fields do not have any components in the direction of propagation.
3. Polarization of EM waves exhibits the oscillating properties of the E-field components of the wave.

4. The wavelength and frequency of the electromagnetic wave is related by the equation  $c = v\lambda$ . Here  $c$  is the speed of the EM wave or light;  $v$  is frequency and  $\lambda$  is the wavelength of the EM wave.
5. When obstructed during propagation, EM waves display scattering properties.

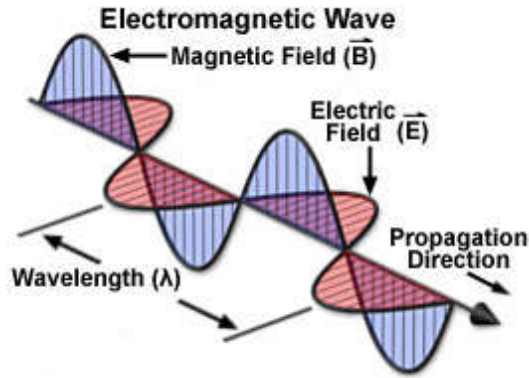


Figure 3.1: A Linearly Polarized Electromagnetic Wave.

### 3.1.1 Maxwell's Equations for a Lossy Dielectric Medium [28]

If the medium is considered lossy, isotropic, homogenous and charge free, then the Maxwell's Equations follow as

$$\nabla \cdot E_s = 0 \quad (3.1)$$

$$\nabla \cdot H_s = 0 \quad (3.2)$$

$$\nabla \cdot E_s = -j\omega\mu H_s \quad (3.3)$$

$$\nabla \cdot H_s = \sigma + j\omega\mu E_s \quad (3.4)$$

Here  $E_s$  and  $H_s$  correspond to the associated Electric field and Magnetic field respectively.

Considering the curl on both sides of equation 3 leads to

$$\nabla^2 E_s - \gamma^2 E_s = 0 \quad (3.5)$$

Similarly, equation 4 can be simplified as,

$$\nabla^2 H_s - \gamma^2 H_s = 0 \quad (3.6)$$

Here  $\gamma$  is known as the propagation constant and is a complex parameter [28]. Its real part  $\alpha$  is known as attenuation constant and its imaginary part  $\beta$  is known as phase constant.

$$\gamma = \alpha + j\beta \quad (3.7)$$

This attenuation constant and phase constant can be simplified further as

$$\alpha = \omega \sqrt{\frac{\mu\epsilon}{2} \left[ \sqrt{1 + \left[\frac{\sigma}{\omega\epsilon}\right]^2} - 1 \right]} \quad (3.8)$$

$$\beta = \omega \sqrt{\frac{\mu\epsilon}{2} \left[ \sqrt{1 + \left[\frac{\sigma}{\omega\epsilon}\right]^2} + 1 \right]} \quad (3.9)$$

### 3.1.2 Scattering Parameters (S- Parameters)

The S-matrix represents a matrix of some complex scattering parameters that help to quantify how RF energy propagates through a multi-port network. These parameters allow us to accurately describe the very complicated networks as simple ‘black boxes’. If an RF signal incidents on one port, some part of it bounces back out of that port, some of it scatters and exits through other ports (and is perhaps even amplified), and some of the signal become nonexistent as electromagnetic radiation or heat.

S-matrices for one, two and three port network are given below [28]:

One port network:  $(S_{11})$

Two port network:  $\begin{pmatrix} S_{11} & S_{12} \\ S_{21} & S_{22} \end{pmatrix}$

Three port network:  $\begin{pmatrix} S_{11} & S_{12} & S_{13} \\ S_{21} & S_{22} & S_{23} \\ S_{31} & S_{32} & S_{33} \end{pmatrix}$

S parameters for a simple two port network are shown in Figure 3.2.

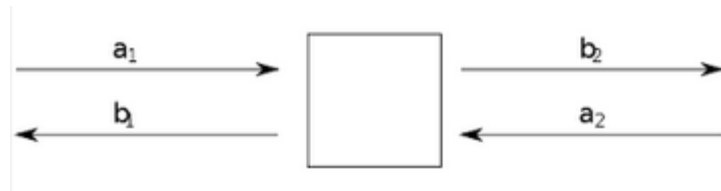


Figure 3.2: A Simple two port network.

Here the incident voltage at each port is ‘a’ and leaving voltage at each port is ‘b’. If the characteristic impedance is  $Z_0$  and considering that each port is terminating at  $Z_0$ , the scattering parameters of the S matrix are defined by [28]:

$$S_{11} = (b_1/a_1); \quad S_{12} = (b_1/a_2); \quad S_{21} = (b_2/a_1); \quad S_{22} = (b_2/a_2).$$

### 3.1.3 Guided Wave Propagation through Dielectric Media

Waveguide: A rectangular waveguide is used in this research work which is excited by a pair of horn antenna. The geometry of the waveguide defines its function. Another important parameter that affects the waveguide’s shape/size is the frequency. The rule of thumb is, the wavelength has to be the same order of the magnitude as the width of the waveguide.

In this study, a rectangular waveguide is used for the guided wave propagation. Rectangular waveguides are one of the earliest types and operate between frequency ranges of 1 GHz to above 220 GHz. This type of waveguide functions as a typical high pass filter. It cannot propagate microwave with frequency lower than its cutoff frequency.

The cut off frequency of a rectangular waveguide is given by [28]

$$f_c = \frac{u'}{2} \sqrt{\left(\frac{m}{a}\right)^2 + \left(\frac{n}{b}\right)^2} \quad (3.10)$$

$$u' = \frac{1}{\sqrt{\epsilon \mu}} \quad (3.11)$$



In free space the electric permittivity is  $\epsilon_0$  and magnetic permeability is  $\mu_0$ , which mean  $\mu'$  will represent the speed of light inside the waveguide. In our initial media (air),  $\epsilon_0=8.85\times 10^{-12}\text{F/m}$  &  $\mu_0=1.257\times 10^{-6}\text{H}\cdot\text{m}^{-1}$ . The 'a' and 'b' dimensions of a rectangular waveguide are shown in Figure 3.3. From here it is clear that only cross section dimensions of the waveguide, parameter 'a' and 'b' affect the cutoff frequency, not the length of the waveguide. The length only affects the power losses.

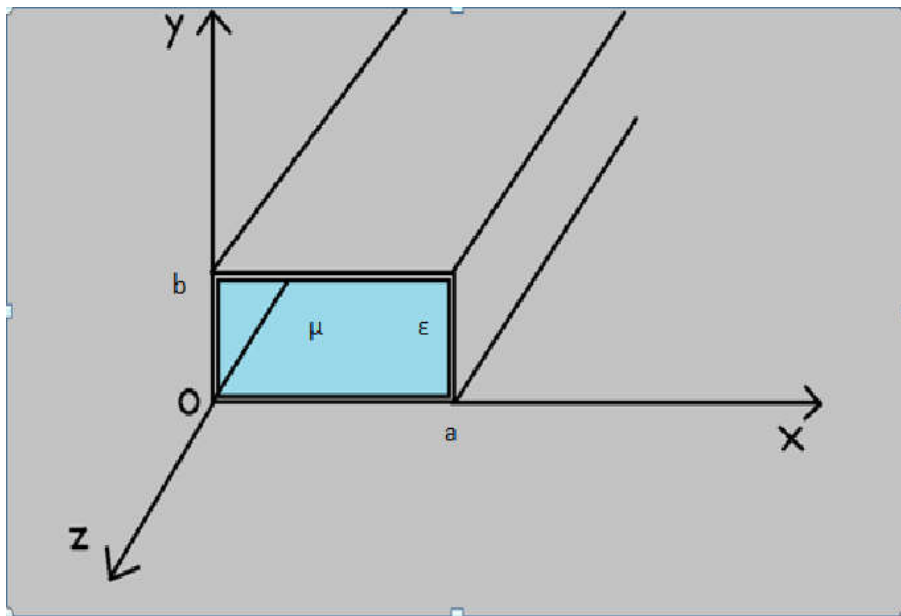


Figure3.3: Rectangular Waveguide.

### 3.1.4 Different Modes for Propagation

Guided EM waves cannot be described as superposition of plane waves that exists in free space. For a particular frequency, an EM wave can be described in terms of different Transverse modes, where each mode has different propagation constant, thus different cutoff frequency[28]. Electromagnetic modes which are responsible for guided propagation are briefly discussed below.

TE Mode:

Here electric field lies in the direction which is perpendicular (transverse) to the direction of propagation.

TM Mode:

Here magnetic field lies in the direction which is perpendicular (transverse) to the direction of propagation.

For rectangular waveguides, 'm' and 'n' represent the number of half wave patterns across the width and height of the waveguide, respectively [28]. For each combination of 'mn' of a particular mode, different cutoff frequency is found. Figure 3.4 shows field patterns of a dominant mode within rectangular and circular waveguides.

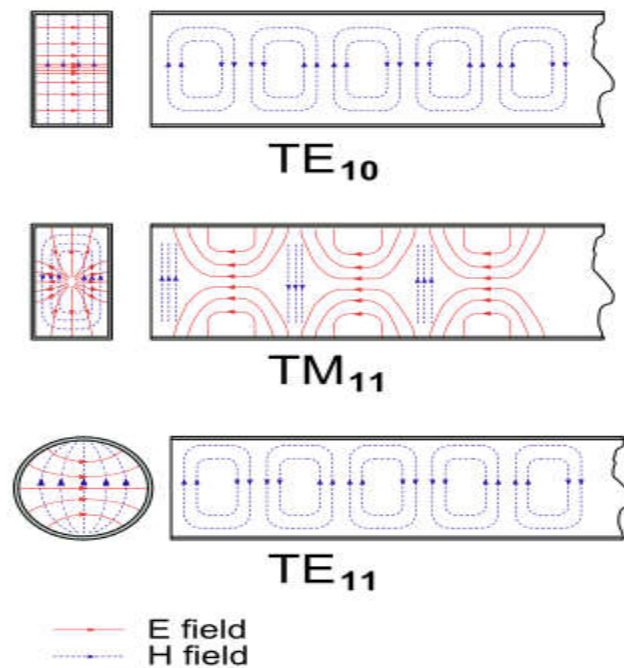


Figure 3.4:Field Patterns of Some Dominant Modes for Waveguides [28].

For non-guided propagation, plane waves propagating with TEM modes are considered. Path loss needs to be calculated to find the attenuation due to sand-dust particles of the propagation path. The equation for pathloss in free space is given by:

$$\text{Free Space Path Loss, FSPL} = \left( \frac{4\pi df}{c} \right)^2 \quad (3.12)$$

Here f is frequency in Hz, d is distance from the transmitter, in meter and c is the speed of light.

## 3.2 Dielectric Properties of Sand

### 3.2.1 Permittivity

EM propagation through sand and dust is generally affected by the dielectric properties of the media. The complex permittivity of sand and dust is given by[28];

$$\epsilon_r = \epsilon' - j \epsilon'' \quad (3.13)$$

Where, the real part  $\epsilon'$  is associated with the stored energy and the imaginary part  $\epsilon''$  represents the dissipated of energy in the sandy-dusty medium.

### 3.2.2 Dielectric Loss Tangent

Dielectric loss tangent is represented as ' $\tan \delta$ ' and expressed as the ratio of the imaginary part to the real part of the complex permittivity  $\epsilon_r$ [28]

$$\tan \delta = \frac{\epsilon''}{\epsilon'} \quad (3.14)$$

It should be noted that, for dielectrics with small value of dielectric loss tangent ( $\delta \ll 1$ ),  $\tan \delta \approx \delta$ . This term normally creates a relationship between distances with the power decay which takes place in the propagation of EM wave.

### 3.3 Soil Taxonomy

The texture of soil varies from region to region in the desert areas all over the world. The United States Department of Agriculture (USDA) and National Cooperative Soil Survey of the United States have classified the types of soil and developed soil taxonomy [31]. This taxonomy provides an elaborate classification of soil types according to several properties and parameters of soil. USDA informs and refines hierarchical classes on the basis of criterion involving soil morphology and laboratory tests. Figure 3.5 presents a summary of the classification of soil in a triangular format.

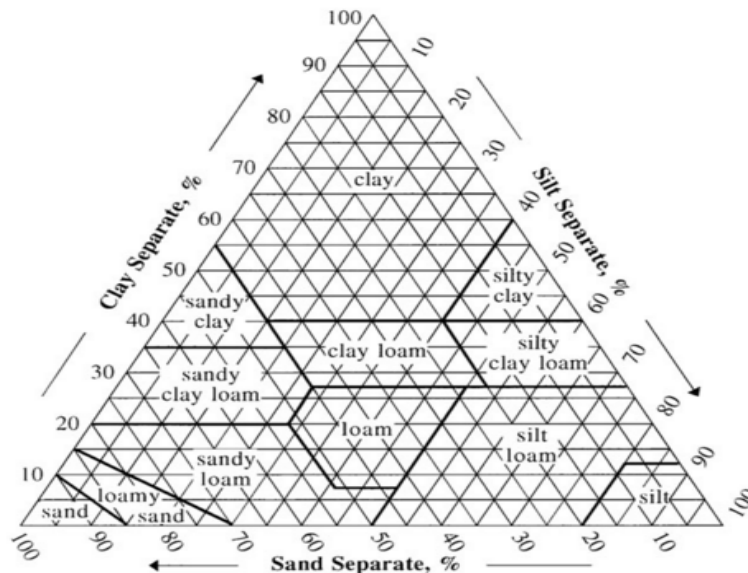


Figure 3.5: Soil texture in triangular format [31].

Most of the sand/dust storms in Saudi Arabia are experienced in areas which are rich in silt and clay. Topographically, dust storms are generated in the low lying regions. This is because of the fact that the prevailing winds are unimpeded by higher terrain. It is also a fact that the world's arid and semi arid regions highly correlate with the major deserts of the world [32]. Figure 3.6 shows a map of the Arabian Peninsula for different grain sizes of soil.

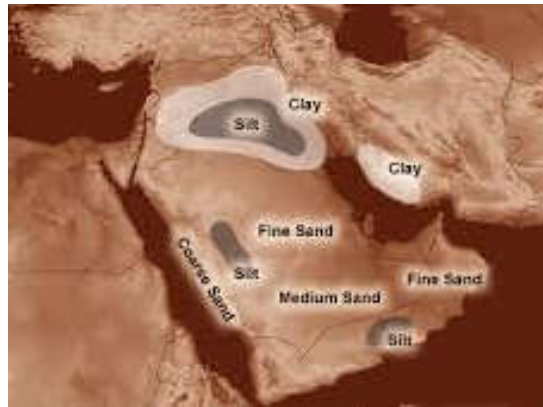


Figure 3.6: Map of soil grain sizes and types in the Middle East [32].

From the Figure 3.6, it is clear that the available sand in the Dhahran region is of Fine Sand type. Thus, the sand samples that are used in this work are collected locally from Dhahran, are also Fine Sand. As this work investigates the X band MW signal propagation through sandy/dusty medium, Table 3.1 shows the Moisture content and dielectric constant of sandy soil for the frequency range of 8-12 GHz (X-band).

Table 3.1: Dielectric constants for different types of soil/sand.

Frequency Range of X band (GHz)	Soil Type	Moisture Content % (H <sub>2</sub> O/g)	Dielectric Constant ( $\epsilon_m^* = \epsilon' - j \epsilon''$ )	Reported By
8-12	Sandy Soil	0	2.53-j0.01	Von Hippel [33]
		3.88	3.6-j0.432	
		16.8	13-j3.77	
	Loamy	0	2.44-j0.003	
		13.7	13.8-j2.484	

### 3.4 High Frequency Structural Simulator (HFSS)

High Frequency Structural Simulator (HFSS) is a software that solves finite element method commercially for electromagnetic structures. It is a product from the renowned software developer company Ansys. This particular software is mostly recognized for designing complex RF electronic circuit elements like filters, transmission lines, antenna etc. This work shall investigate propagation of MW signal in several arrangements. The basic steps in designing such an arrangement are provided below:

- At first, the software model is designed. This includes designing objects, antennas, selecting medium etc.
- After that, boundaries are assigned for the medium. In this work, simulation scenarios include guided and non-guided propagation. For simulating guided environment, 'Perfect E' boundaries are used. And to represent the non-

guided simulation environment, the boundaries of the test box are assigned as ‘Radiation’ boundaries.

- Next the excitations are assigned, i.e. antennas are generated to record responses. These assigning of excitations are done by selecting faces of the object in concern.
- Then, the simulation profile is selected. This includes choosing frequency ranges of interest.
- Finally choosing the type of graph is necessary. The parameters of interest are chosen to observe the simulation responses.

Figure 3.7 shows an example of a rectangular waveguide constructed in HFSS. Here the boundaries are chosen as ‘Perfect E’.

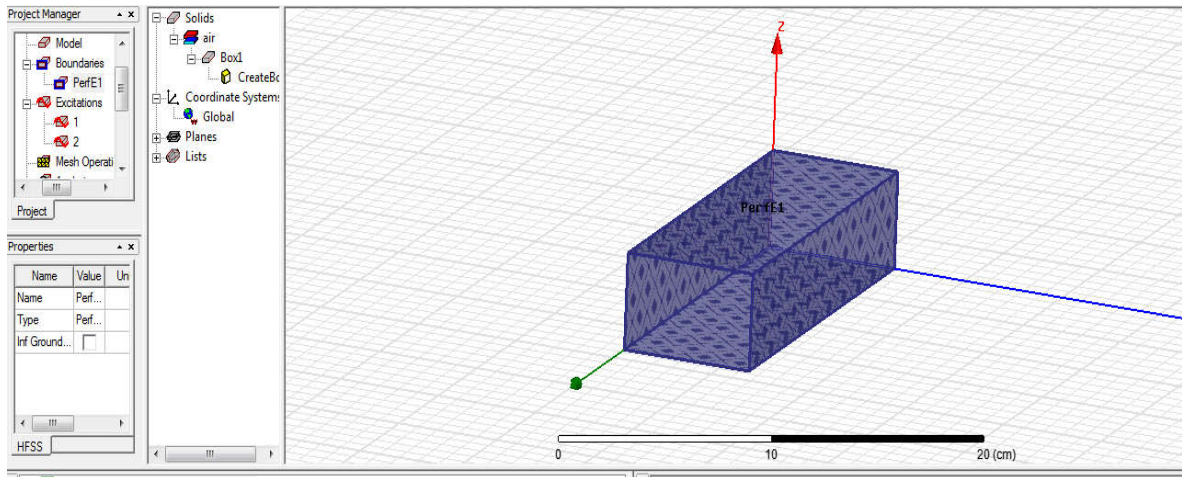


Figure3.7: Simulated model of rectangular Waveguide in HFSS.

Figure 3.8 shows one of the assigned wave ports to one side of the constructed waveguide.

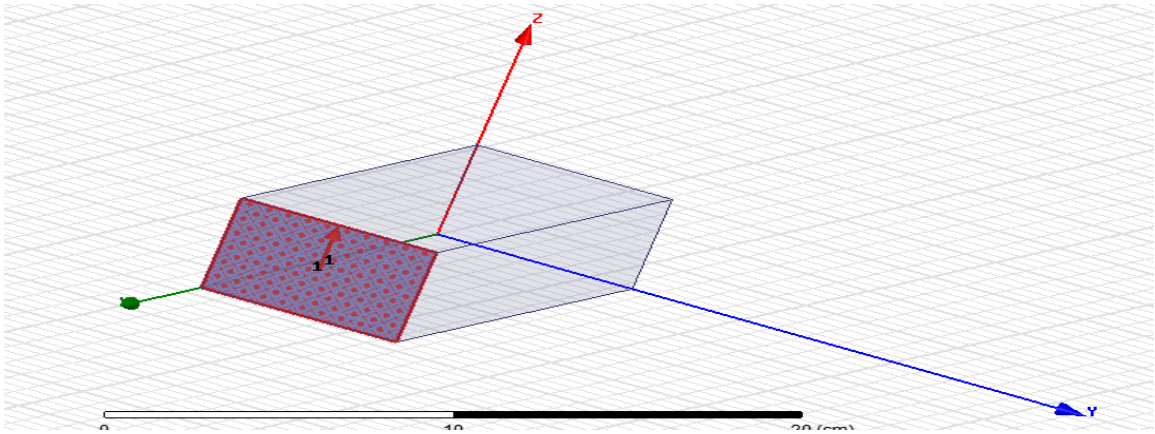


Figure 3.8: Wave port in construction for simulating S parameter responses for the waveguide.

Once the setup is completed, choosing appropriate material inside the waveguide can be done by selecting properties to assign materials. This window consists of a set of predetermined materials; even new materials can be created too.

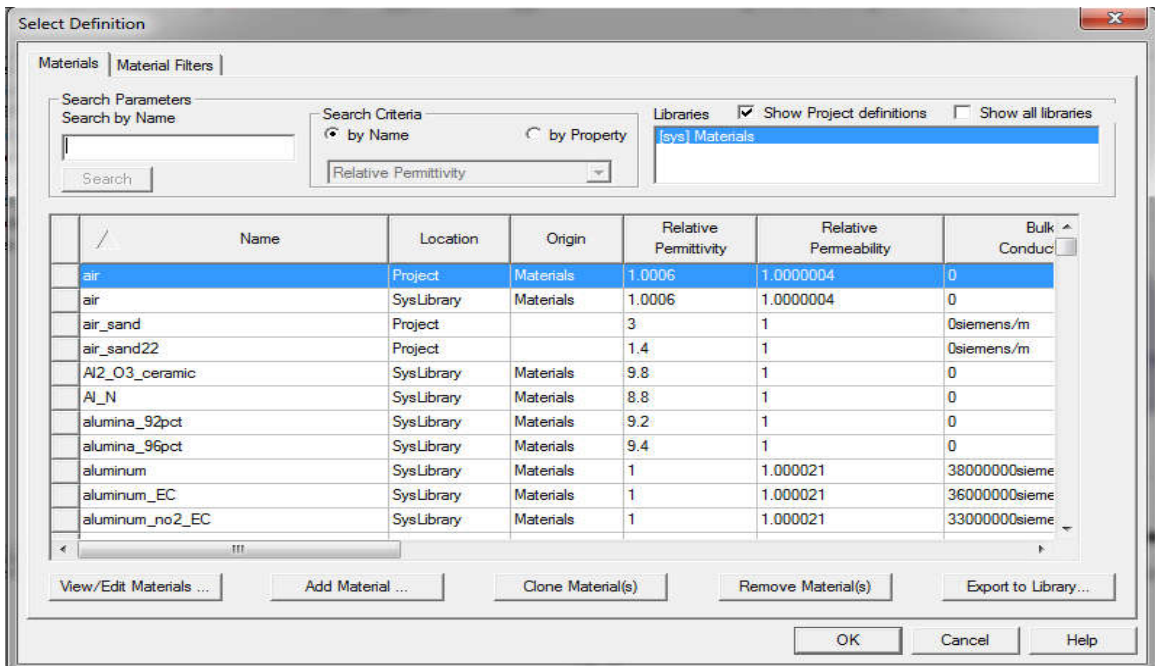


Figure 3.9: Material selection in HFSS simulation software.



Then the simulation profile is chosen as per requirement. For frequency sweep, a range needs to be selected. A solution frequency is chosen as well and the minimum number of passes needs to be fixed as well.

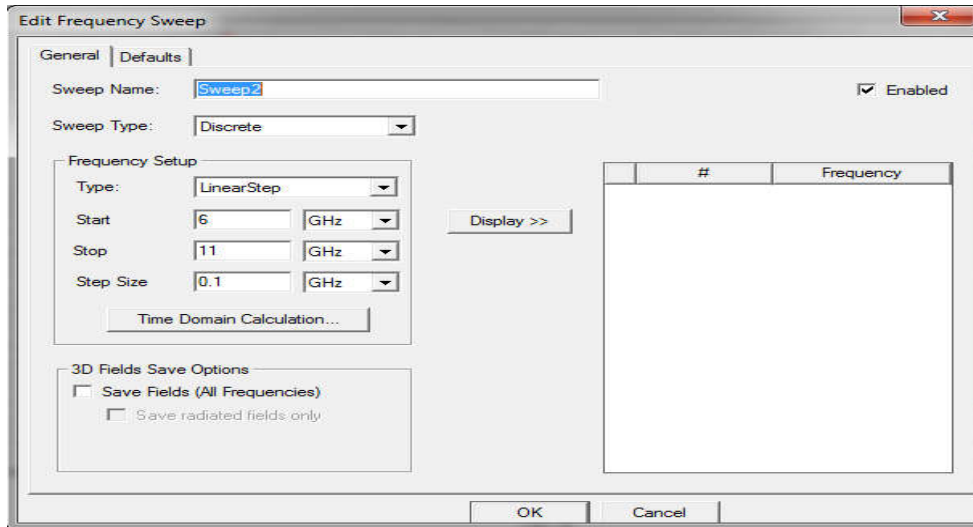


Figure 3.10: Window for choosing frequency sweep.

Once the simulation is completed, necessary results can be obtained by choosing the appropriate plot in the post processor menu (like S-parameters, Radiation patterns, input Impedance etc).

## CHAPTER 4

# EXPERIMENTAL VERIFICATION OF THE SIMULATION MODEL OF SANDY/DUSTY MEDIA

### 4.1 Propagation through Guided Media

As an initial investigation, attenuation of microwave signal propagating through sand-dust filled rectangular waveguide is experimentally measured. These results will be used later to tune the software-simulation-model before using it for investigating non-guided propagation. This experimental setup used a coaxially fed rectangular waveguide with dimensions of  $a = 16.4$  cm and  $b = 8.2$  cm. The length of the waveguide was 78 cm. The schematic diagram and the rectangular waveguide setup used in this experiment are shown in Figure 4.1 and Figure 4.2 respectively.

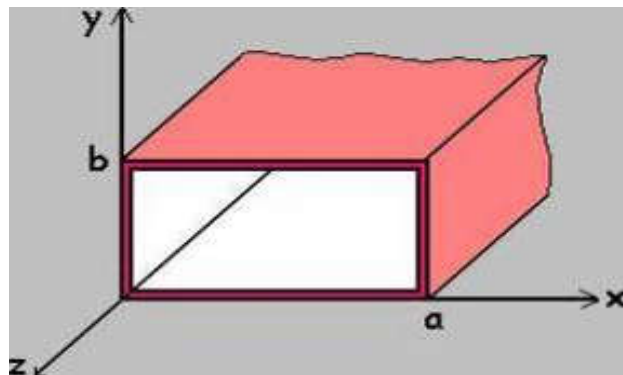


Figure 4.1: Schematic diagram of a rectangular waveguide.



Figure 4.2: Photograph of the set up that was used for guided measurements.

Using a blower fan, a mixture of air-dust and sand-dust media were created within the waveguide before using the network analyzer to monitor the scattering parameters. But this measurement requires knowledge about the modes operating inside the waveguide.

#### **4.1.1 Propagation Modes**

It is well known that rectangular waveguides need either E or H field component in the direction of propagation. Thus, it supports the propagation of  $TM_{mn}$  (transverse magnetic) and  $TE_{mn}$  (transverse electric) modes, where the 'm' and 'n' are the number of half cycle variations of the fields in the x and y directions, respectively. The cut-off frequency of the rectangular waveguide was calculated using equation (3) of chapter 3 and is tabulated in Table 4.1.

Table 4.1: The Cut off frequencies (GHz) of rectangular waveguide.

	<b>n=0</b>	<b>n=1</b>	<b>n=2</b>	<b>n=3</b>	<b>n=4</b>	<b>n=5</b>
<b>m=0</b>		1.83	3.66	5.48	7.31	9.14
<b>m=1</b>	0.91	2.04	3.77	5.56	7.37	9.19
<b>m=2</b>	1.83	2.59	4.09	5.78	7.54	9.32
<b>m=3</b>	2.74	3.30	4.57	6.13	7.81	9.54
<b>m=4</b>	3.65	4.09	5.17	6.59	8.18	9.84
<b>m=5</b>	4.57	4.92	5.85	7.13	8.62	10.22

Here, for the Transverse Electric (TE) modes  $n, m \geq 0$  ( $n \neq m \neq 0$ ), while for the Transverse Magnetic TM modes,  $n, m \geq 1$ . The parameters ‘a’ and ‘b’ were chosen as 16.4 cm and 8.2 cm respectively, as per the dimension of the rectangular waveguide that we used in the laboratory.

#### **4.1.2 Horn Antenna**

Although coaxial feed was adequate to excite the guided microwave propagation through air-sand-dust filled rectangular waveguide, non-guided propagation through sandy/dusty media required antennas. A horn antenna, made of tapered rectangular waveguide section, is an efficient radiator of microwave signal. At the same time the shape also helps to minimize reflection due to improved impedance matching throughout a very wide frequency range. A schematic diagram of a rectangular waveguide antenna is shown in Figure 4.3. The cut off frequencies of this antenna depend on the rectangular

waveguide that excites metal horn, and the values can be found similarly as mentioned in the earlier sub-section 4.1.1.

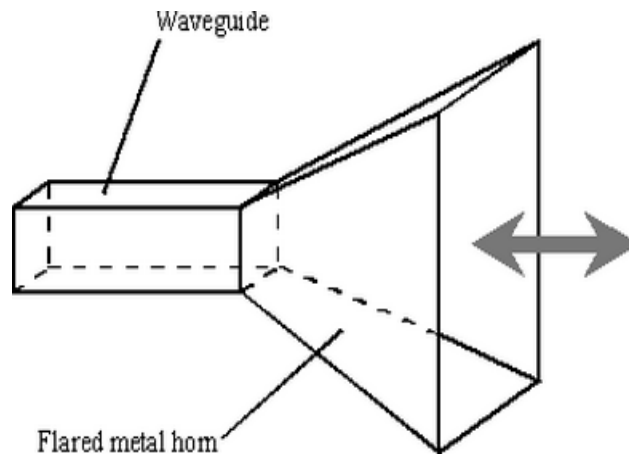


Figure 4.3: Schematic diagram of a Horn antenna.



Figure 4.4: Photograph of the Horn antenna used to excite the waveguide.

The small rectangular waveguide associated with this horn antenna had dimensions of  $a=2.3$  cm and  $b=1.1$  cm. Our frequency of interest in this particular measurement was 8-10 GHz. By calculating other cut off frequencies with different modes, it is seen that only  $TE_{10}$  mode is propagating. Using these values of 'a' and 'b' the cut off frequency for the  $TE_{10}$  mode was found to be 6.517 GHz (for the horn antenna).

### **4.1.3 Sieve Analysis to Separate Sand/Dust Samples**

To fill the waveguide with air-dust or air-sand mixture, sand and dust samples are needed. Sieve analysis is widely used to separate the sand particles according to their particle size. This is important, as the attenuation of the propagating signal needs to be related to different vertical layers of the sand storm, which normally has sand particles of different sizes and intensity. The sieve analysis is used here to separate three sand-dust samples with different particle sizes. The machine used for this process is shown in Figure 4.5. Figures 4.6 and 4.7 show the Sieve analysis process, implemented by the mechanical multi-compartment vibrator. The machine separates the sand samples using pre-selected trays that allow the sand particles with certain diameters to travel to the lower compartments. Once the sieve analysis is completed, sand-dust samples with different particle sizes are collected from different compartments of the machine. From the literature survey, the concerned range for particle size is up to 150  $\mu\text{m}$ . The machine that was used for Sieve analysis had the minimum filter of a diameter of 90  $\mu\text{m}$ . So we collected some sand samples and separated particles under three categories: diameter of 90  $\mu\text{m}$ , 125  $\mu\text{m}$ , and 150  $\mu\text{m}$ . These separated samples of sand are shown in Figure 4.8.



Figure 4.5: The mechanical shaker used for Sieve Analysis.



Figure 4.6: Loading sand samples in the Sieve analysis setup.



Figure 4.7: Separation of sand samples through mechanical shaking.



Figure 4.8: Separated sand samples of diameter 90  $\mu\text{m}$ , 125  $\mu\text{m}$ , and 150  $\mu\text{m}$ .

After sieve analysis was done, the resultant sand samples of different sizes were collected in separate jars in order to use it in the experiments.



#### **4.1.4 Experimental Set-up for Propagation through Rectangular W/G**

A two port Vector Analyzer (HP8510) is used to observe the attenuation of the microwave signal, propagating through a rectangular waveguide filled with air-sand and air-dust media. To simulate a sand-dust storm, several air-holes were embedded within the rectangular waveguide to introduce pressured air-flow. Consequently, the waveguide was filled with desired air-sand or air-dust mixture. Care was taken to avoid leakage from the waveguide. Since the volume of the waveguide and the quantity of sand particles were known, the concentration of the particles can be calculated. The experimental setup of air-sand/air-dust filled waveguide with pressured air flow is shown in Figure 4.9. The connections of the network analyzer to the transmitting and receiving sections of the waveguide are also shown. Note that optimized coaxial probes are used in the figure to excite (port 1) and receive (port 2) microwave signals. The attenuation due to single mode and multi-mode propagation through the air-sand and air-dust filled waveguide is observed by monitoring the S-parameter responses. The vector network analyzer allowed the measurement of magnitude and phase responses of the reflection ( $S_{11}$ ) and transmission ( $S_{21}$ ) parameters to demonstrate how the propagating microwave signal is affected by different sand-dust samples.



Figure 4.9: Inducing Sand storm within the rectangular waveguide.

#### 4.1.5 Experimental Results for Waveguide Excited by Coaxial Feed

For two frequencies (1.4 GHz and 8 GHz), the measured S-parameters for guided microwave propagation through air-sand/air-dust media are listed in Table 4.2. Since the cut-off frequency of the waveguide is 0.91 GHz, the frequencies of 1.4 and 8 GHz are selected to observe the attenuation for single and multi-mode microwave excitations, respectively. It is clear from this table that air-sand mixture introduces extra attenuation in both frequencies. As increasing frequency increases the electrical length of the microwave signal, the resulted attenuation of the propagation signal is much larger. Also the dielectric properties of the air-sand media have larger effect on the high frequency signal (8 GHz) compared to low frequency signal (1.4 GHz). Since the coaxial probes were designed to optimally excite the waveguide at 1 GHz, the observed S-parameters for 1.4 GHz signal was more accurate compared to 8 GHz signal. The responses shown in the higher frequencies are less stable than that of lower frequencies. Also the results at

high frequency were difficult to reproduce. To overcome this situation, the rectangular waveguide with air-sand and air-dust filling was excited using horn antennas.

Table 4.2: Experimental results for guided propagation excited by coaxial probe.

Frequency (GHz)	Condition	S <sub>11</sub> (dB)	S <sub>21</sub> (dB)
1.4	Air filled waveguide	-14.88	-0.229
	Air-Sand filled waveguide	-10.02	-0.34
8	Air filled waveguide	-19.1	-8.8
	Air-Sand filled waveguide	-5.5	-12.5

#### 4.1.6 Experimental Results for Waveguide Excited by Horn Antenna

A pair of rectangular horn antennas was used to excite the rectangular waveguide. Care was taken to avoid leakage during pressurized air flow, which creates the air-sand or air-dust mixture. Using the same technique of the previous section, network analyzer was used to measure the S-parameters (magnitude and phase) of the propagating microwave signal.

The air-sand and air-dust mixture was created using specified quantity of the three sand-dust samples with particle sizes 90  $\mu\text{m}$ , 125  $\mu\text{m}$  and 150  $\mu\text{m}$  (separated earlier using sieve test). For a signal frequency of 9 GHz, Figures 4.10, 4.11 and 4.12 display the transmission responses (S<sub>21</sub>) of the air-only, air-dust and air-sand filled waveguide for sand samples of 90  $\mu\text{m}$ , 125  $\mu\text{m}$  and 150  $\mu\text{m}$ , respectively.

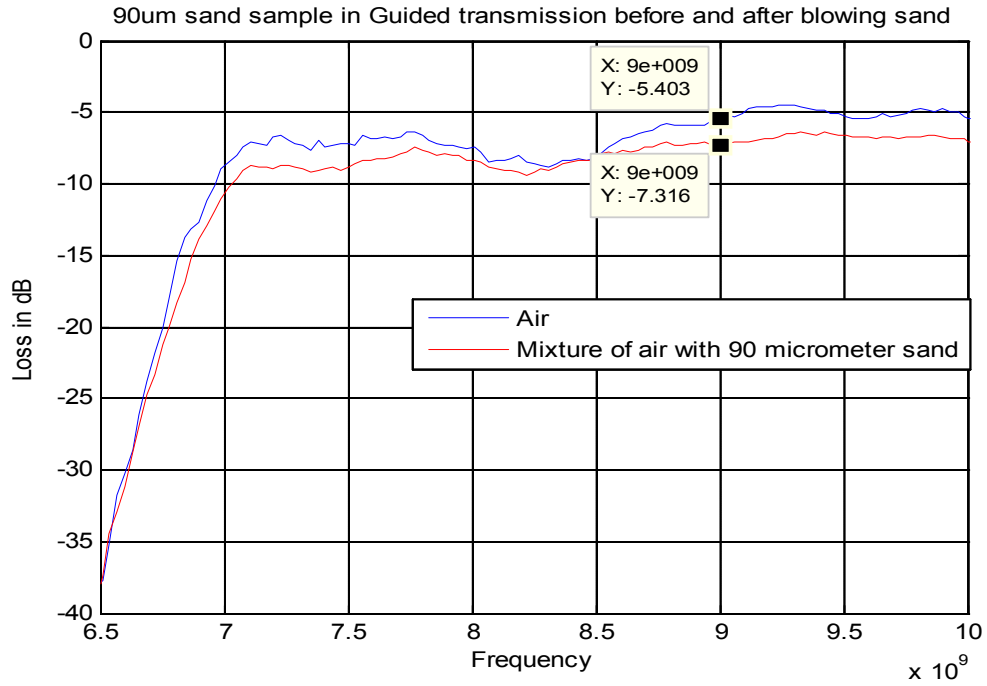


Figure 4.10: Measurement of S-parameters for guided propagation with 90 μm sand samples.

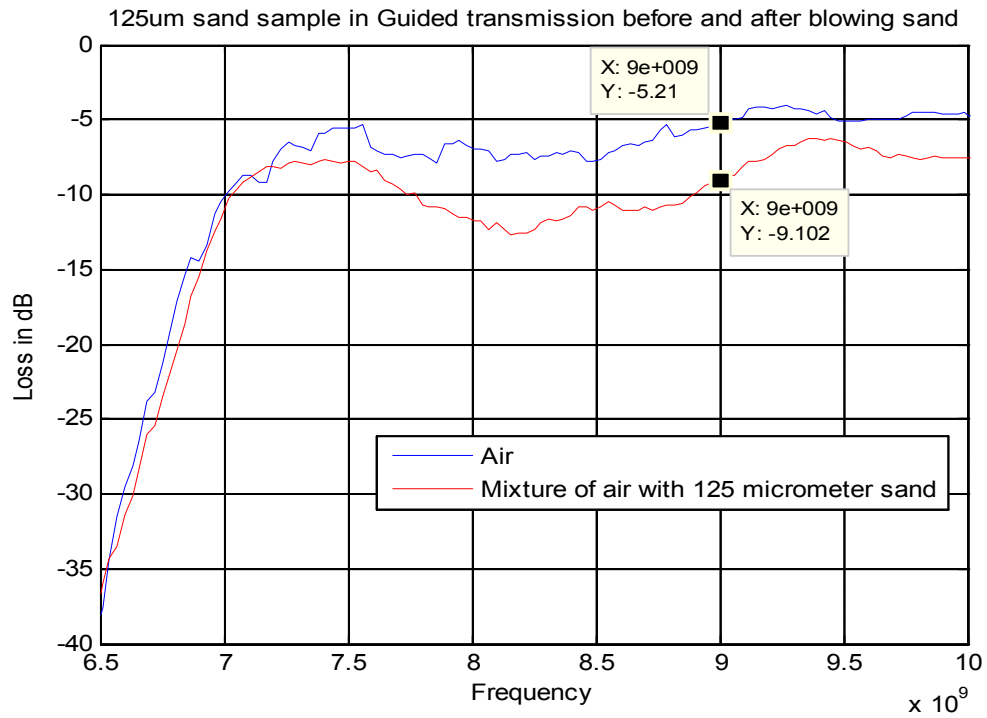


Figure 4.11: Measurement of S-parameters for guided propagation with 125 μm sand samples.

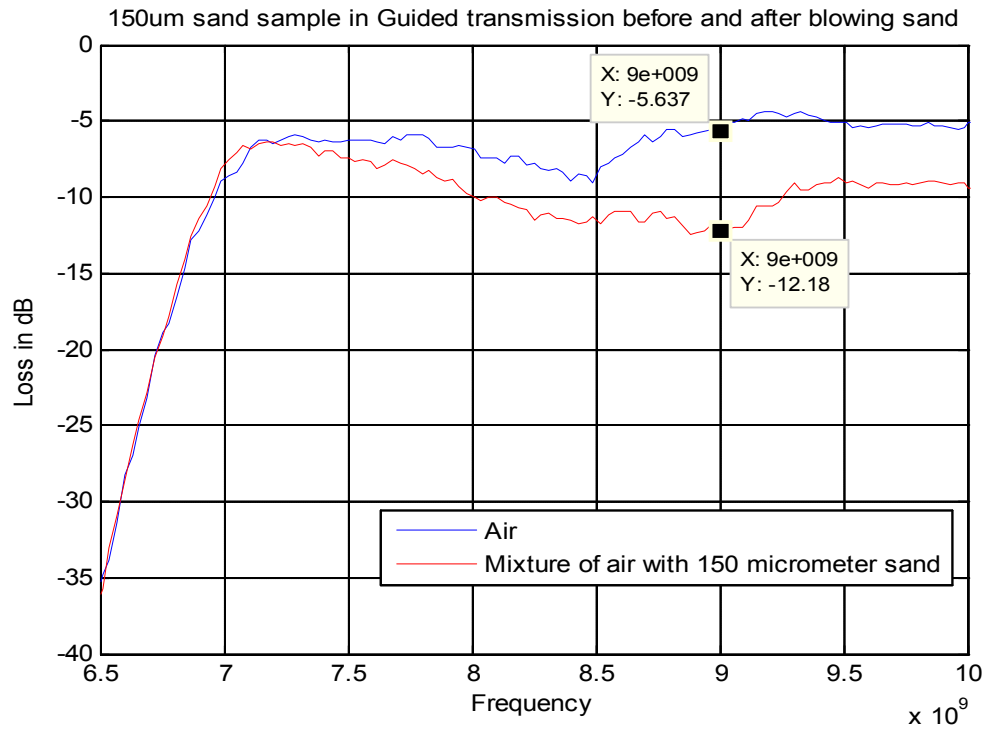


Figure 4.12: Measurement of S-parameters for guided propagation with 150  $\mu$ m sand samples.

Experimental findings are given here in tabular format for guided propagation for different size of sand particles. Here frequency of interest is 9 GHz.

Table 4.3: Experimental results for guided propagation excited by horn antenna.

For sand sample with diameter of:	90 $\mu$ m	125 $\mu$ m	150 $\mu$ m
S21 for Waveguide filled with Air only	-5.4 dB	-5.21 dB	-5.637 dB
S21 for Waveguide filled with air-sand/air-dust	-7.32 dB	-9.102 dB	-12.18 dB
Attenuation of the EM wave due to sand/dust	1.92 dB	3.892 dB	6.543 dB

From the above results, it is clear that losses due to the presence of sand with air are increasing with the increase in particle size. This is expected as increase in particle size increases the effective dielectric constant of the transmission medium, which causes more scattering and absorption of propagating microwave signal.

#### **4.1.7 Simulation Results for Guided Propagation using HFSS**

Since filling the waveguide with air-sand and air-dust mixtures are difficult without causing leakage, carrying out multiple experimental observation are difficult. So a validated simulator model of similar setup is proposed here for the investigation of change in attenuation, polarization of the microwave signal due to air-sand and air-dust media. The professional software used in the research work was called: High Frequency Structural Simulator (**HFSS**).

This software is mostly used to analyze microwave properties of EM propagation and devices including transmission line, filters, antennas etc. The simulation model of the measurement-setup is shown in Figure 4.13. The steps for creating the software model of a rectangular waveguide terminated by transmitter and receiver horns are briefly discussed here. At first, the structure is drawn according to the size of the given waveguide. After that the waveguide medium is selected by assigning values for relative permittivity and loss tangent. Then the metallic waveguide boundaries are assigned by choosing Perfect-E boundaries for the simulated waveguide. An air box with radiation boundaries (hidden from Figure 4.13) are integrated around the waveguide to implement perfectly matched layers. The simulation setup is created by setting 1.4 GHz as solution frequency and then a frequency sweep to obtain S-parameter responses for desired

frequencies (1-10 GHz). The finite element solver required specifying an error-margin and final passes to limit simulation time depending on satisfying either criterion. The electromagnetic wave is excited using ports assigned to selected boundary. Integration line is available to define different excitation modes, as required. In the later part of the simulation, the model includes a complicated horn antenna, attached with the rectangular waveguide to minimize simulation error (not shown in figure 4.13). Once the model is complete, simulation is initiated to obtain the S parameters responses of the propagating microwave signal through sand-dust-air filled rectangular waveguide.

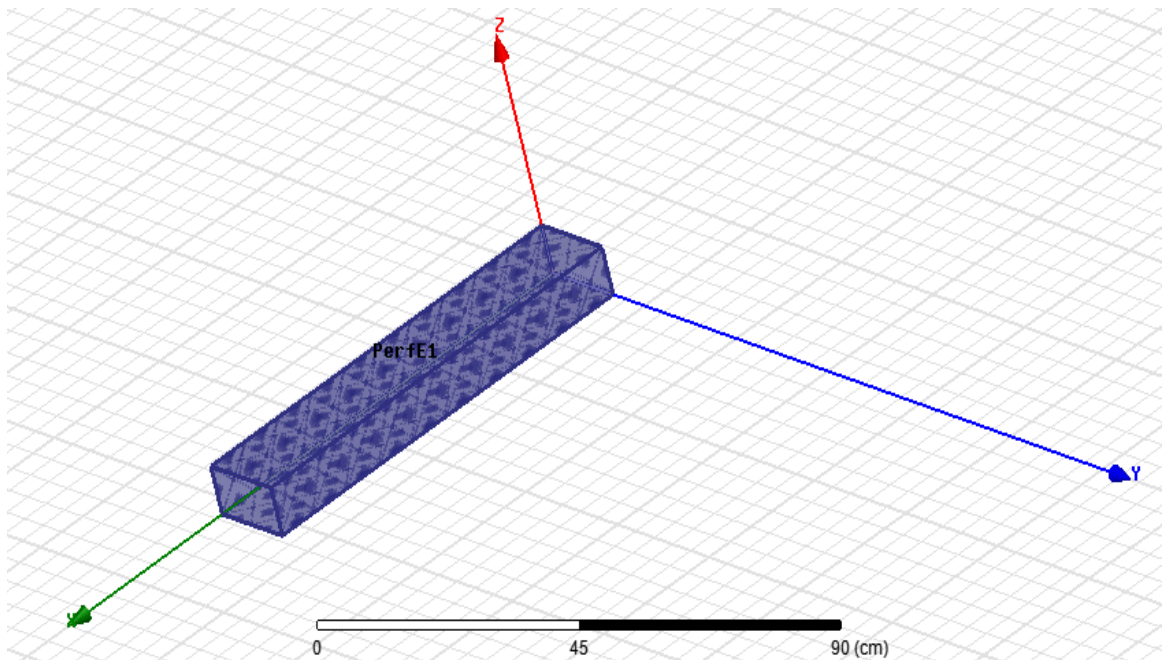


Figure 4.13: Air-sand/air-dust filled waveguide, excited by ideal port.

Using this setup, several simulations are conducted and compared with the experimental results (Table 4.2) to validate the software model by optimizing meshing parameter, port setup, dielectric loss tangent, permittivity etc. It is observed that for sand sample with effective permittivity  $\epsilon_{eff} = 3$  and dielectric loss  $\tan \delta = 0.002$ , the simulated results best matched experimental S-parameter responses, as tabulated in Table 4.4. Note that

these simulated results are comparable to experimental responses listed in Table 4.2. Once validated, the simulation model can now be used to simulated complex non-guided propagation of microwave through air-sand and air-dust filled media.

Table 4.4: Simulated S parameters for rectangular waveguide.

Frequency (GHz)	Type	S21 (dB)
1.4	Air only	0
	Sand air mixture	-0.38
8	Air only	-1.5
	Sand air mixture	-21.1

Due to the influences of the guiding structures, this simulation method cannot be used for non-guided setup. Similar simulation analysis is done later in this chapter for the case of non-guided propagation by changing the properties of the structure which contains the medium for signal propagation.

## 4.2 Propagation through Non Guided Media

For non guided propagation measurements, a 4 mm thick plastic box is fabricated to accommodate the sand-dust storm within a laboratory environment. The dimension of the box was chosen as 80 cm x 60 cm x 60 cm. The box is shown in Figure 4.14.





Figure 4.14: Plastic Box built for investigation of non guided propagation.

This dimension was best suited for achieving required concentration of the air-sand or air-dust mixture using the existing quantity of the sand samples. A pair of horn antennas is also used here to excite and receive the microwave signals. The schematic diagram of the measurement setup used to monitor the effects of the air-sand and air-dust media on the propagating microwave signal is shown in Figure 4.15.

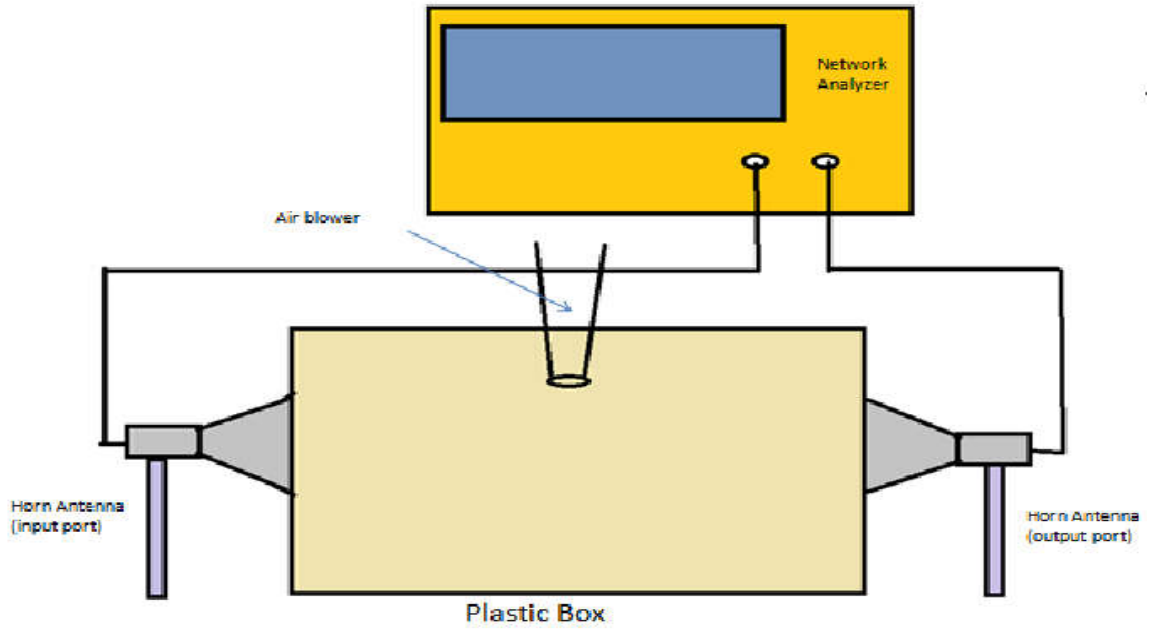


Figure 4.15: Schematic diagram for non-guided attenuation measurement setup.



Figure 4.16: Non-guided attenuation measurement setup with loaded sand samples of 300 gm.

Using optimally placed air-ducts (holes), pressured air flow is circulated through the box to achieve sand/dust storm like dielectric media. Multiple air blowers are used for this purpose and the ducts are positioned to maintain uniform air-sand or air-dust mixture through the propagation path of the microwave signal. Filter strips are used to design air outlets, which are carefully positioned within the box, allowed only the air to pass without letting sand/dust particles to escape the plastic box.

At the beginning of the experiment, horn antennas are optimally positioned in both sides of the plastic box to record initial transmission and reflection responses of the X-band microwave signal, propagating through air-plastic media. This measurement is later used as a reference value to obtain the attenuation of the microwave signal due to air-sand or air-dust dielectric contents of the box. This initial measurement is also used to align the antenna positions, to excite X-band microwave signals, throughout the measurements.



Figure 4.17: Propagation through air-sand media with concentration of  $1.04 \text{ kg/m}^3$ .

Once the measurement setup is ready, sand/dust samples are loaded within the box. The mass of the sand/dust samples that was put inside the box was chosen as 300 grams throughout the experiment. Multiple strong blowers are used to mix the sand /dust sample thoroughly to simulate a sand storm like dielectric environment within the box. Figure 4.17 shows a scenario showing the measurement taking process with sand/dust samples with sand concentration of  $1.04 \text{ kg/m}^3$ . Using horn antennas, microwave signal is excited within the box to monitor scattering and attenuation of the propagating microwave signal for different samples and even for different concentrations.

To make the air-sand and air-dust mixture as uniform as possible, air-blowing through air-vent holes were used. The circulation of sand inside the box was clearly visible. After that the measurements of the losses were taken through the network analyzer, by blowing air through a heavy air blower. Here all of the sand samples were used separately, i.e. sand sample of diameter  $90 \text{ }\mu\text{m}$ ,  $125 \text{ }\mu\text{m}$ , and  $150 \text{ }\mu\text{m}$ . Although the S- parameter readings for X-band is recorded, the frequency of interest in this observation is 9 GHz. This allowed the comparison of simulated results with experimental data.

#### **4.2.1 Experimental Results for Non-guided Propagation**

The S-parameter values, which were observed with the help of network analyzer, are plotted using MATLAB software. The superimposed plots for three different sand samples are plotted in Figure 4.18. It should be noted that the mass density for these experimental findings were taken for a sand concentration of  $1.04 \text{ kg/m}^3$  in each case.

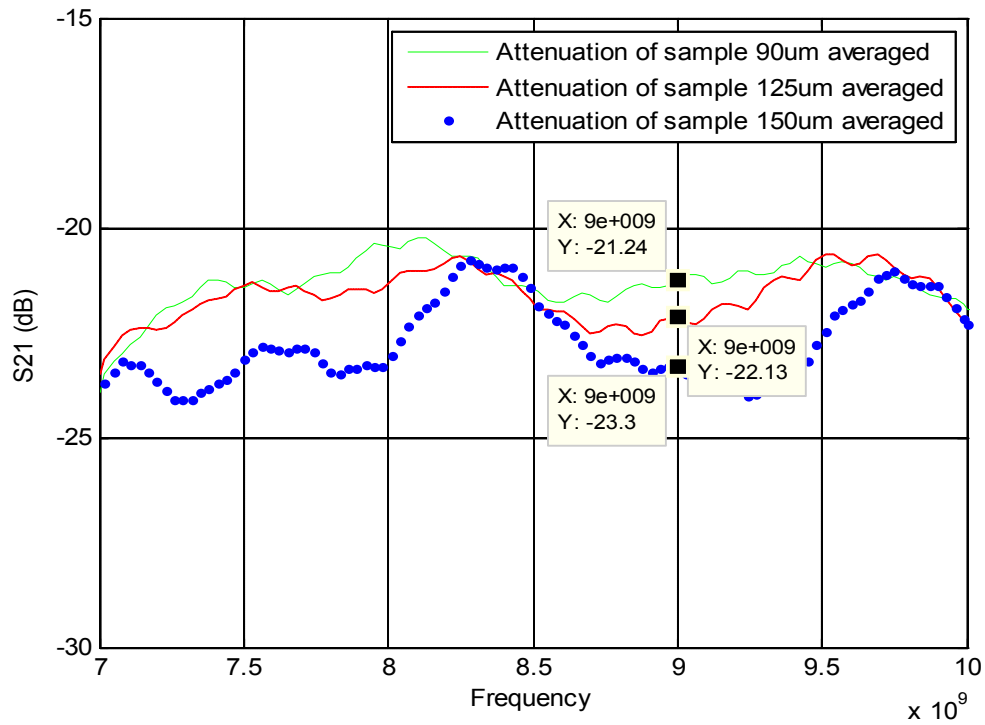


Figure 4.18: Comparison of measured attenuation of MW signal at 9 GHz, propagating through three sand samples.

In the above Figure, the losses for three different sizes of sand (see cursor values) are shown and here it becomes clear that loss is higher for the bigger size of sand particles. For 150  $\mu\text{m}$  diameter sand particles, the losses are particularly higher than that of the other two.

## 4.2.2 Simulation Results for Non-guided Propagation

In this part of the research work, the simulation model of the horn antenna is used to excite the air-sand or air-dust filled rectangular waveguide. As it is mentioned earlier, the cutoff frequency obtained from the dimension of the waveguide used in the horn antenna is 6.51 GHz. The frequency of interest is kept as 9 GHz. The software model is created to be replica of the experimental setup, as shown in Figure 4.19. Note that it is much easier to align the horn antennas in

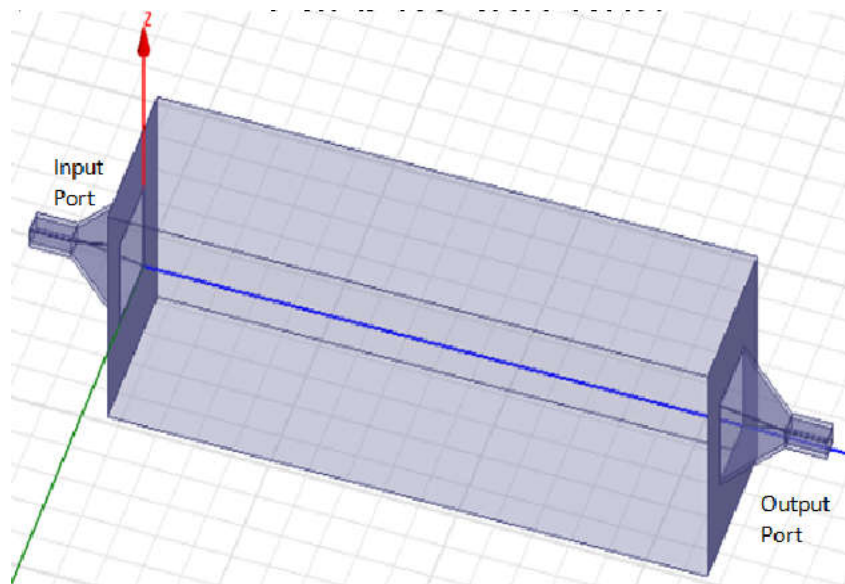


Figure 4.19: Simulator model of air-sand or air-dust filled box excited by horn antenna.

simulation model than it is in experimental setup. The main reason for doing this simulation is to compare the simulated responses with experimental data to determine the effective permittivity of the air-sand and air-dust mixture within the box. This is achieved by approximating a uniform dielectric constant and thus finding the simulated S-parameters, until they match with the experimental observed S-parameters. For the

given sand samples, the effective permittivity that produced equivalent scattering responses varied between  $2 < \epsilon_{eff} < 3$ . Note that the simulated models assumed standard value of dielectric loss tangent constant of 0.002. Figure 4.20 displays the transmission properties of the equivalent homogeneous media.

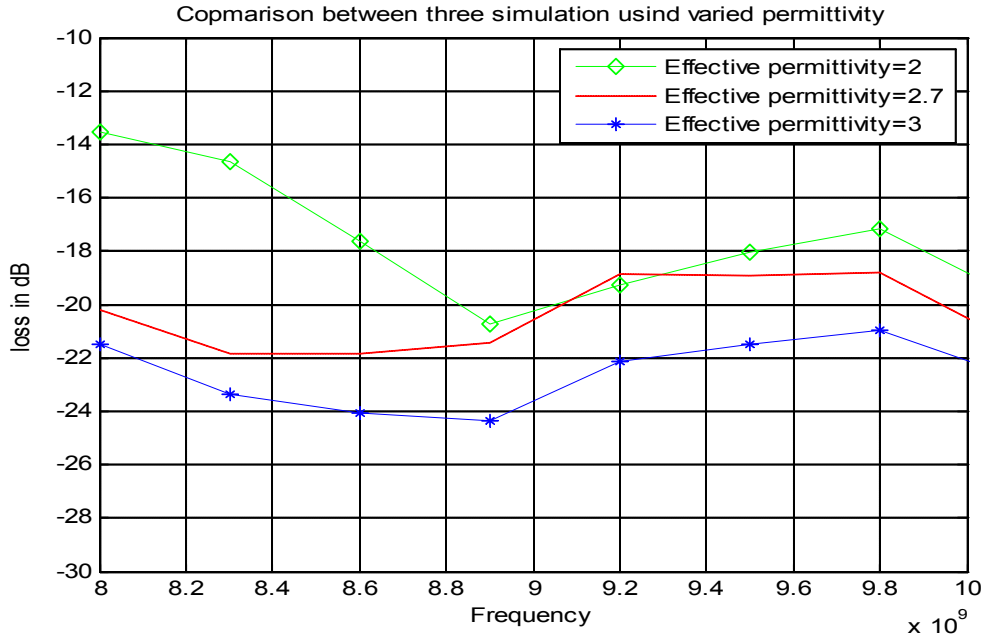


Figure 4.20: Comparing losses for different  $\epsilon_{eff}$ , for non guided propagation.

Comparison between experimental and simulation results for non-guided propagation is performed in this section. The simulated back calculations provided the  $\epsilon_{eff}$ , values of 2, 2.7 and 3 for dust-sand samples with particle sizes of 90  $\mu\text{m}$ , 125  $\mu\text{m}$ , and 150  $\mu\text{m}$ , respectively. The superimposed experimental and simulated results are presented in Figures 4.21 to 4.23. These figures also validate the simulation model. In the following chapter, this validated model is used to investigate how microwave signal is affected by the sand-dust particle size, orientation, shape and concentration.

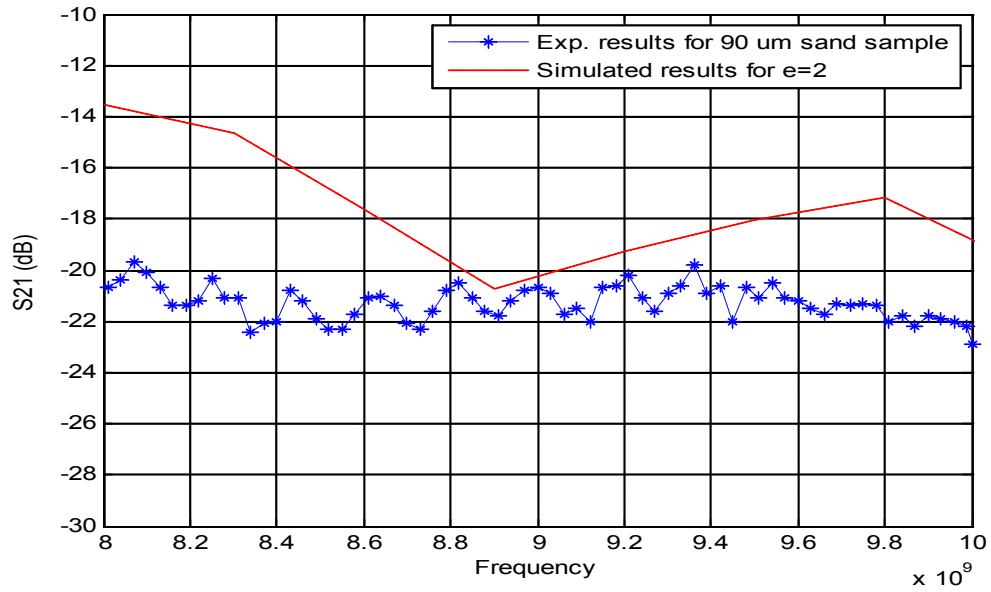


Figure 4.21: Comparing simulation of  $\epsilon_{eff}=2$  with the experimental results using 90  $\mu\text{m}$  particles.

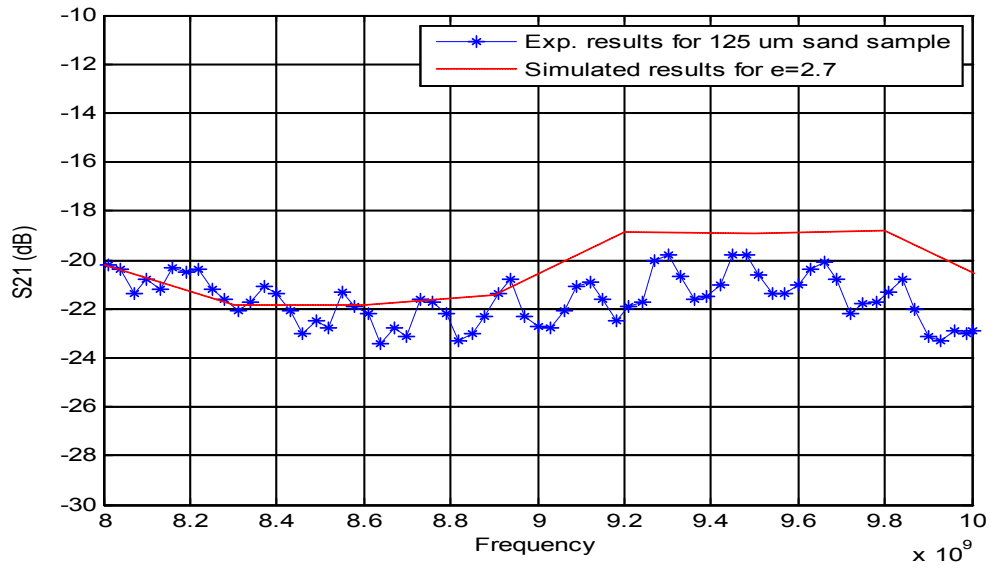


Figure 4.22: Comparing simulation of  $\epsilon_{eff}=2.7$  with the experimental results using 125  $\mu\text{m}$  particles.



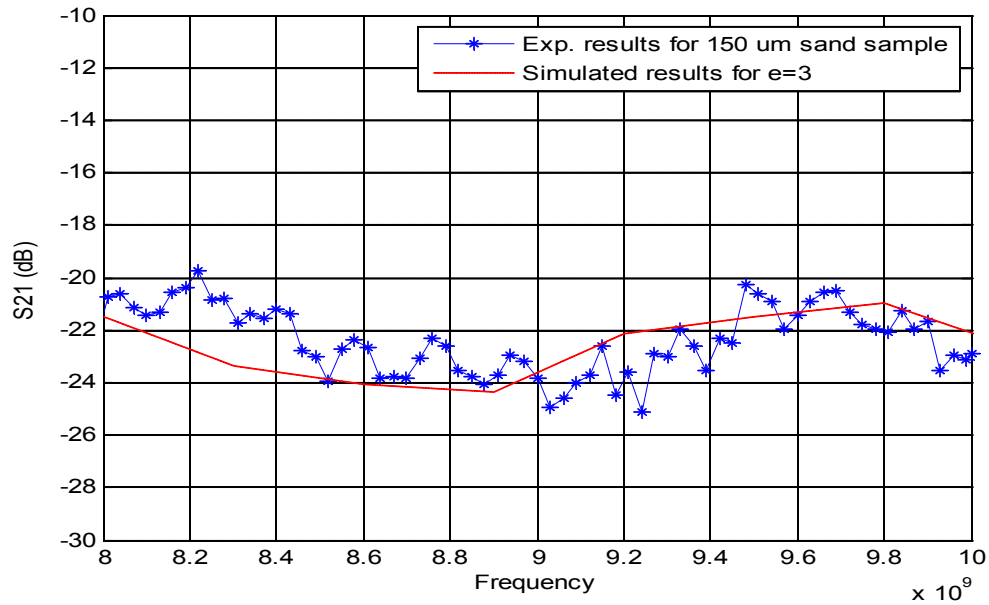


Figure 4.23: Comparing simulation of  $\epsilon_{eff}=3$  with the experimental results using 150  $\mu\text{m}$  particles.

Among the three comparisons, the results which are shown in Figure 4.21 reproduce the worst match. Though at 9 GHz the results of simulation is pretty close to experimental value. Figures 4.22 and 4.23 show that though there are much variations in the experimental results which were collected using real time observations, the basic trend match while comparing it with the simulated results. The findings in these two figures show that the experimentally obtained S parameters can be observed through simulation that varies effective permittivity of the medium of propagation.

The works which are discussed in this chapter enabled us to choose effective permittivity value for sand particles which is to be used later in this thesis for simulation purpose.

## **CHAPTER 5**

### **SIMULATOR BASED ANALYSIS OF MW**

### **PROPAGATION THROUGH SANDY/DUSTY**

### **MEDIA**

#### **5.1 Background of the Modified Simulation Model**

The study of microwave (MW) propagation through sand/dust storm relies heavily on the experimental data on visibility measurements. The review of the literature in chapter 2 revealed that the process of collecting visibility data is often difficult and random to draw conclusions. In the research work of Al Hafid et al. [9], which was conducted using 13 GHz signal on the outskirts of Baghdad city, found that the fading depth of the received MW signals are much larger than that of the predicted results. Similarly, when J.W. Ryde [10] dealt with radar reflectivity, he found the losses to be very little for dust storms. But this conclusion came for the frequencies that are at the lower end of the microwave frequency spectrum. Ghobrial [12] made some estimation for X-band MW signals and demonstrated different attenuation for different particle size and distribution of the sand-dust particles. Then there comes other parameters like the particle geometry, humidity ratio etc. All these indicate one thing that experimental data could provide an actual scenario for a particular case, but in general, when it comes to predicting an overall

estimation of signal quality or losses, various parameters are associated with it and a general conclusion is very difficult to draw. In these circumstances, a validated simulation model could be very much welcome to predict the nature of microwave link under sand/dust storm. This model could be used to predict the scattering and polarization changes of the propagating microwave signal due to some certain individual parameters, like particle geometry, size and concentration.

The experimental results of chapter 4 provided a clear indication on the pattern of the signal behavior, while propagating through different layers of sand storm i.e. for different particle radius of sand. The later part of chapter 4 introduced the simulated results for the similar setup that was used for the experimental results. But those simulations only demonstrated the signal losses due to effective permittivity of the media, as air-sand or air-dust mixture was approximated as a uniform media. Since that simulation did not take account of parameters like the size of the sand particles, the scattering and polarization effects of EM waves were not accurately predicted.

In this chapter, how MW signal is affected due to size and concentration of sand/dust particles are analyzed. Figure 5.1 shows the set up used for the software model which is created by the professional software HFSS (High Frequency Structural Simulator). This model will be used to analyze how microwave signal is affected by the parameters like particle size, shape, and concentration of sand particles.

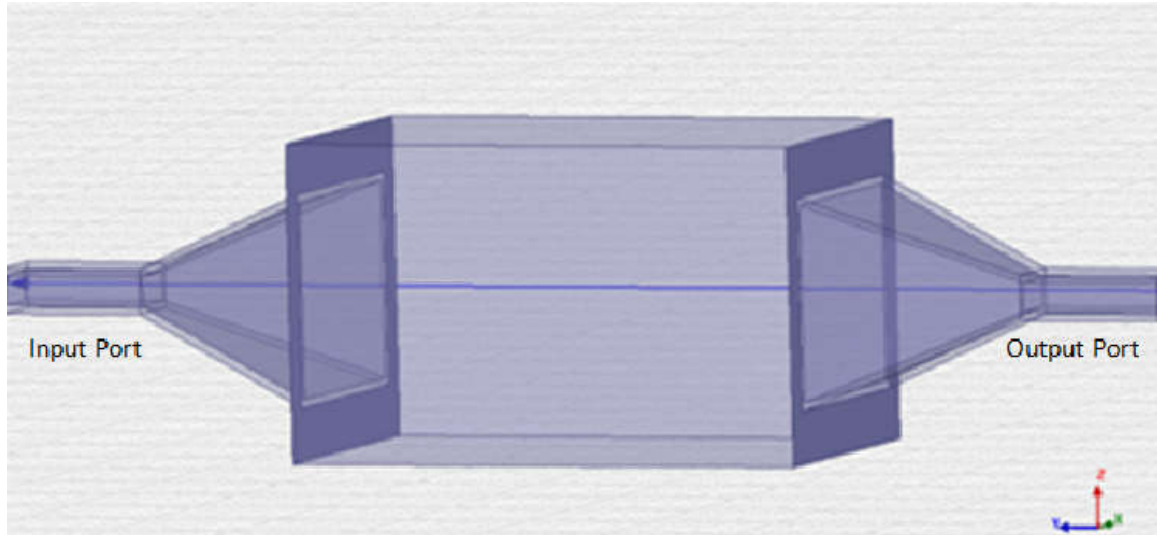


Figure 5.1: Simulated propagation box between a pair of horn antennas.

The size of the scaled box is selected to be: length 20 cm, height 12 cm and width 12 cm. This particular dimension is different from that of previous chapter to reduce simulation time. For this particular box, the simulation runtime is about 1-1.5 days for a computer having about 16 GB of RAM. Whereas, the box that was made for simulation in chapter 4 took upto 2-3 days for a single run. Once the box is modeled, the sand/dust particle shapes are introduced within the box. The added advantage of this particular model is that it includes the convenience of choosing the geometry of the particle we are analyzing. As per literature review, the most commonly used shapes for sand particles are the circular shape and the ellipsoid shape. Thus this model shall analyze these two shapes. At the beginning, regular and symmetric distributions are used, though later, simulation scenario consisted of only random distribution of sand particles. The results given for random distribution differed a bit from the results given for regular distribution of sand spheres, as expected. But here we considered only the random particles distribution since it is

obvious that the real time scenario would include sand distribution as random. One particular example of such simulation is given below.

## 5.2 Modified Simulation Model with Sand/Dust Samples

The simulation model with sand/dust samples and the process of recording the S-parameter responses are briefly discussed below.

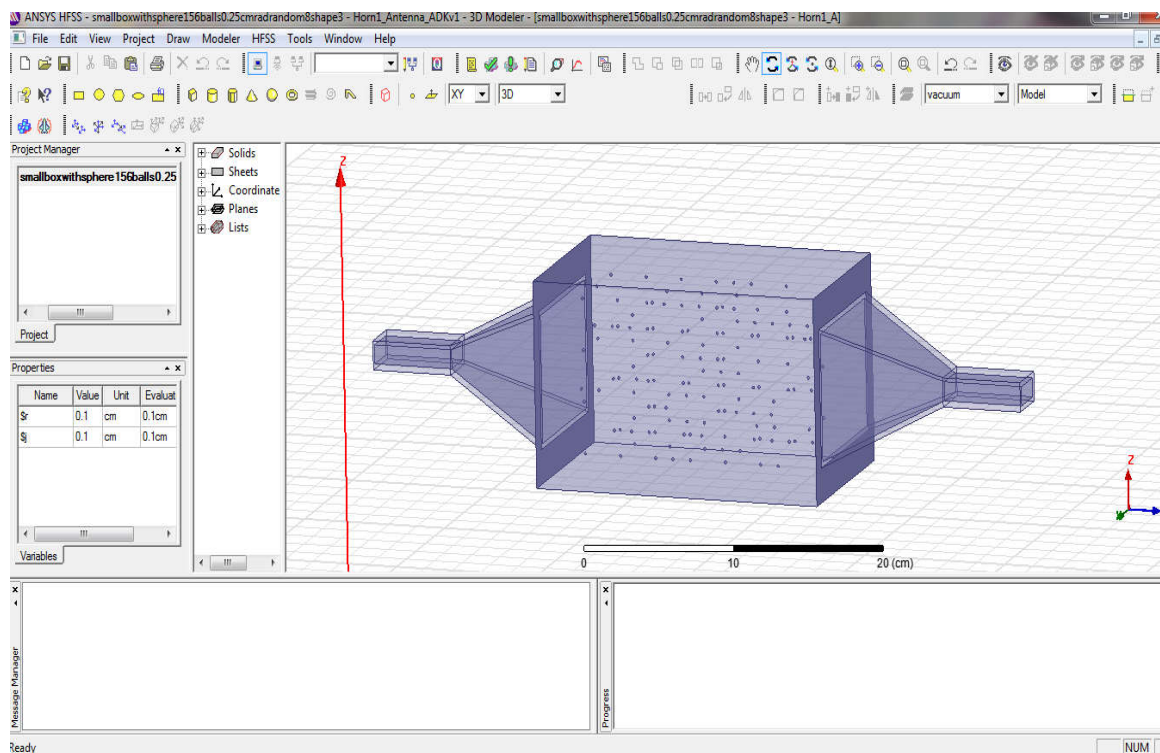


Figure 5.2: Simulator model with 105 circular,  $\epsilon_{\text{eff}}=3$  and randomly distributed sand-dust samples, for particle radius of 0.10 cm.

The model is excited with X-band frequency sweep and the responses are recorded by measuring the scattering parameters of two port network ( $S_{21}$  and  $S_{11}$ ). The  $S_{21}$  parameter is of particular interest, as it represents the transmission response. For the setup of Figure 5.2, the following reflection and transmission responses are observed.

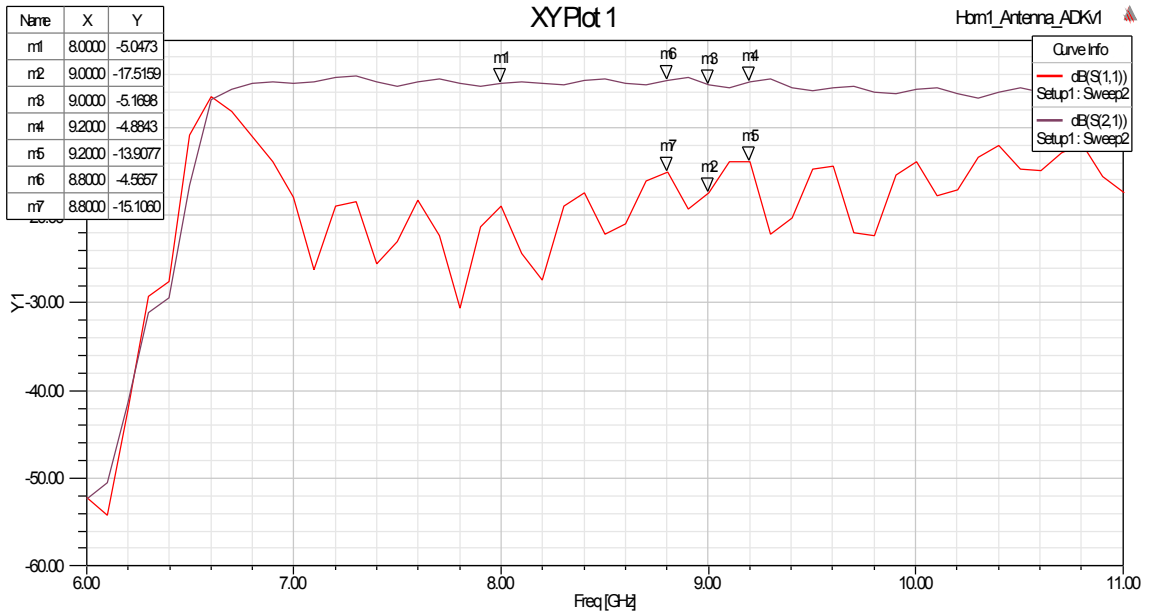


Figure 5.3: The magnitude response of S21 and S11 for 105 spherical shaped sand particles.

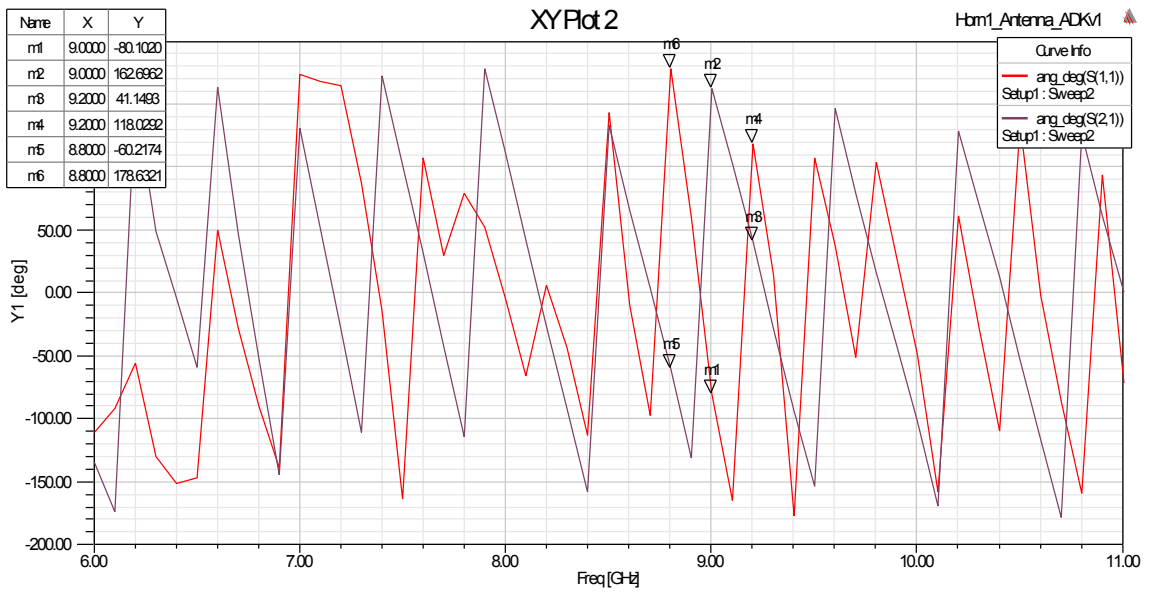


Figure 5.4: The phase response of S21 and S11 for 105 spherical shaped sand particles.

Although the measurements of phase responses are also recorded, only the magnitude parts of the transmission responses are analyzed.

### **5.2.1 Investigated Parameters of the Sand-Dust Media**

The objective of this simulation model is to observe the effects the sandy/dusty media have on MW propagation, when parameters like particle shape, size and concentration vary. For the purpose of modeling, two of the most popular shapes have been investigated as particle shape. They are spherical and ellipsoid. For each kind of shape, two important parameters are varied here:

- a. Radius of the sand particles.
- b. Sand concentration.

### **5.3 Investigation for Spherical Shaped Sand Particles**

From the literature it is found that, spherical shape is one of the most popular shapes of sand particles. Thus, at first, spheres are chosen as sand particles in the simulation model. The particles which were put into the set up which was shown in Figure 5.2 are spherical.

#### **5.3.1 For Different Size of Sand Particles**

One of the principle objectives of this research work has been to study the effects of different sized sand particles on the microwave signals that suffer attenuation under sand and dust storm. In this simulation modeling, the radius of the sphere shaped sand particles is tested to see the effects on the transmission responses ( $S_{21}$ ). The radius values chosen are: 0.015 cm, 0.05 cm, 0.10 cm, 0.25 cm, 0.38 cm and 0.50 cm. In real sand storms, particles are found to be having radii up to 0.02 cm. For simulation model, the results are

more accurate if we can include numerous sand spheres of having such tiny radius. But in reality, it is extremely difficult to include thousands of models of tiny sand particles manually. Thus sand particle sizes bigger than 0.02 cm are considered.

The transmission responses ( $S_{21}$ ) are observed for different sand concentration i.e. different number of sand particles per unit box. The size of the unit box is mentioned earlier. The calculated scattering parameters( $S_{21}$ ) at 9 GHz for three different sand concentrations are presented in Figures 5.5 to 5.7.

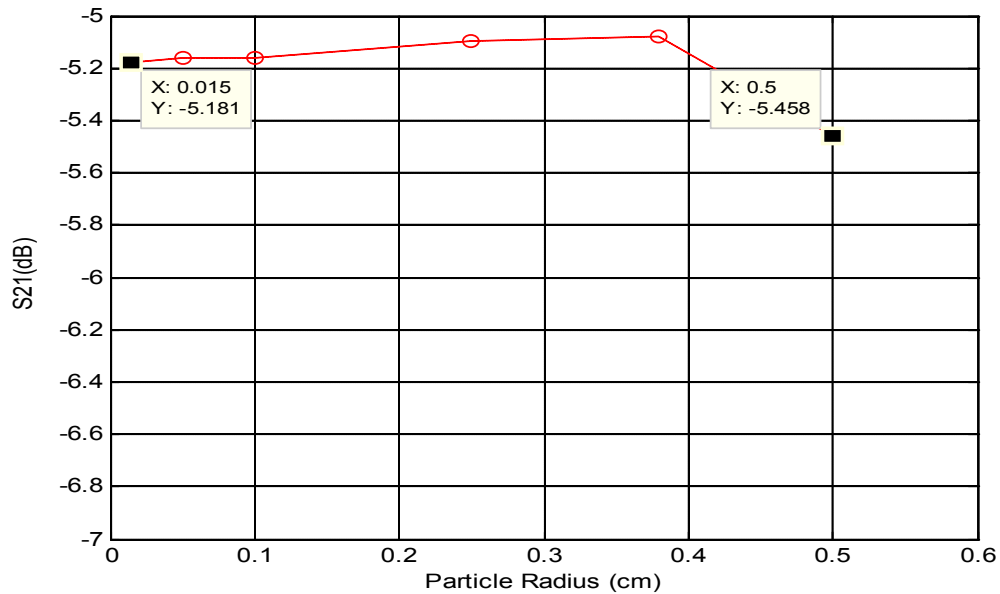


Figure 5.5:  $S_{21}$  response for sand concentration of 63 spherical particles/unit-box.

This result shows that there is a considerable increase in losses when the particle radius is large (0.5 cm) compared to small radius (0.015 cm). Though the in between values are not following a particular pattern that would indicate higher losses for greater particle



sizes. This may be due to smaller concentration of the sand samples, as explained later in this section.

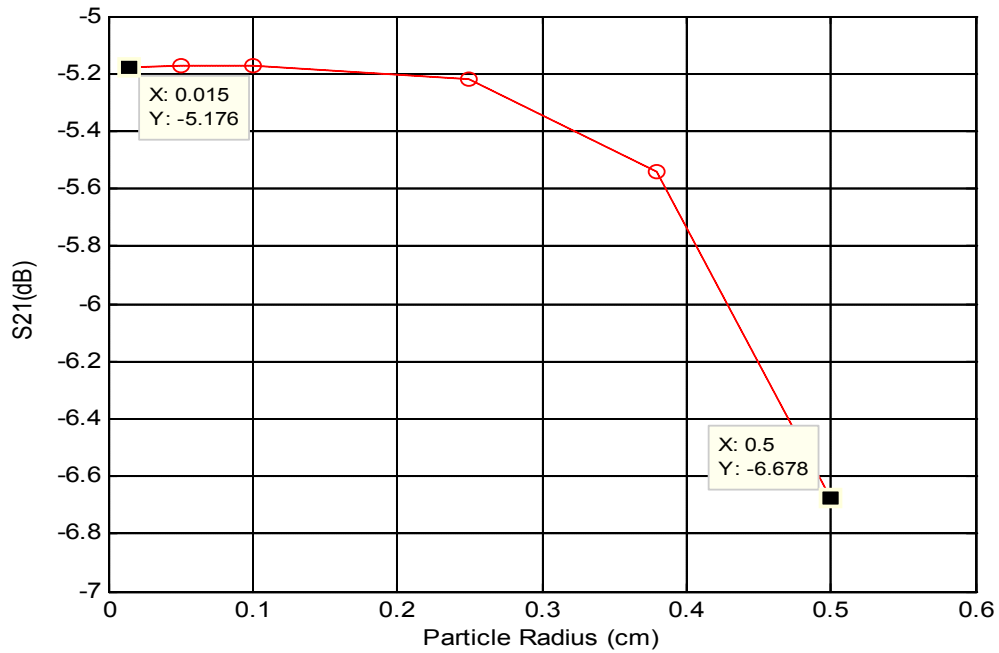


Figure 5.6: S21 response for sand concentration of 105 spherical sand particles /unit-box.

For sand concentration of 105 spheres, we can see a nice pattern indicating higher losses with the increase in particle radius. As expected, there is a considerable rise in the losses for greater particle radii like 0.38 cm and 0.5 cm.

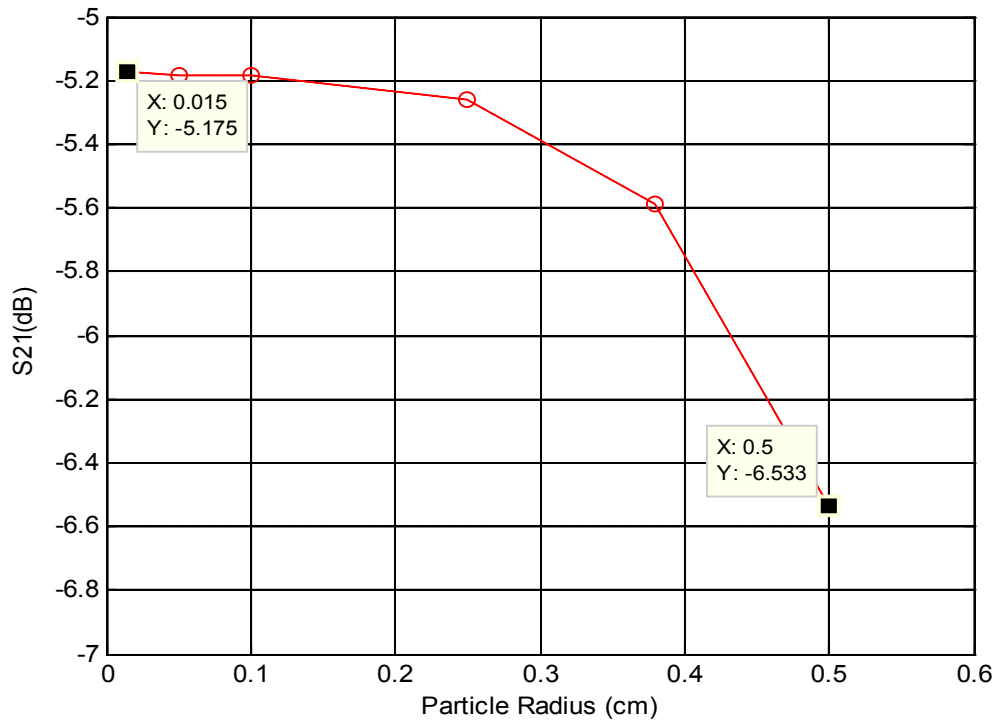


Figure 5.7:  $S_{21}$  response for sand concentration of 135 spherical sand particles /unit-box.

Results for sand concentration of 135 sand spheres are similar to the one that is for 105 sand spheres. The rising pattern here too is visible and clear as in the previous figure. After analyzing all the results given in Figures 5.5-5.7, it is clear that larger sand particles lead to greater loss. This is because increasing the sand particles increases the effective permittivity of the propagating media in addition to increase in scattering. These cause the reduction in received signal in output port. This finding also maintains the same pattern of the results which were experimentally observed in chapter 4. The results in Figure 5.5 which shows  $S_{21}$  response for 63 sand spheres indicate that increased particles radius does not always lead to greater transmission loss. Though the differences found for different particle radius is very minimal, then again the trend in the result do not show

greater losses for greater particle size. This result pattern is found even when the responses are taken at other frequencies, e.g. 8.8 GHz and 9.2 GHz. Thus the limitation of this particular simulation model lies such that for very low sand concentration, where the responses differ very less with each other, the results could be random in nature and might not bring a particular pattern.

### **5.3.2 For Different Concentration of Sand Particles**

After studying the effects of variation in the size of the sphere shaped sand particles, the second case is tried, where the sand concentration is varied and observation of the effects on the attenuation is made. To represent the variance in sand concentration, different numbers of sand spheres are considered. The numbers are randomly selected to be: 63, 105 and 135. The orientation of the sand spheres is always kept random. It is clear that the case with 135 sphere shaped sand particles can be considered about 2 times more concentrated sand than that of the case, which take account 63 sphere shaped sand particles.

Like the previous sub-section, here too, the measurements are made at 9.0 GHz and the simulated S-parameter (S21) responses are shown in Figures 5.8 to 5.11. The simulated results for frequencies of 8.8 GHz and 9.2 GHz are observed and they demonstrated similar characteristics as well. It is clear from these figures that higher sand concentration leads to a greater loss in transmission response.

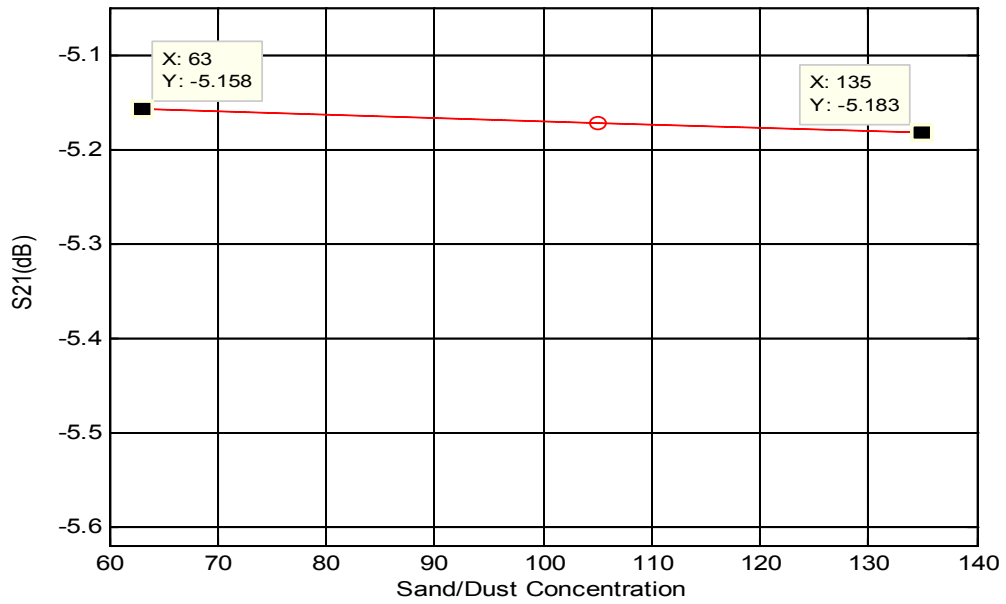


Figure 5.8: S21 response for spherical sand radius of 0.05 cm

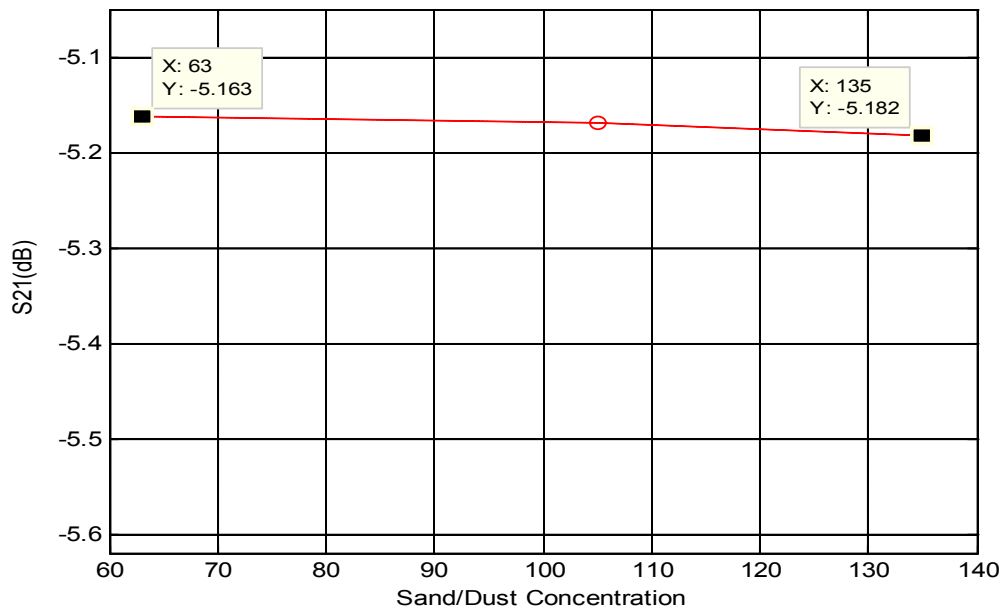


Figure 5.9: S21 response for spherical sand radius of 0.10 cm.

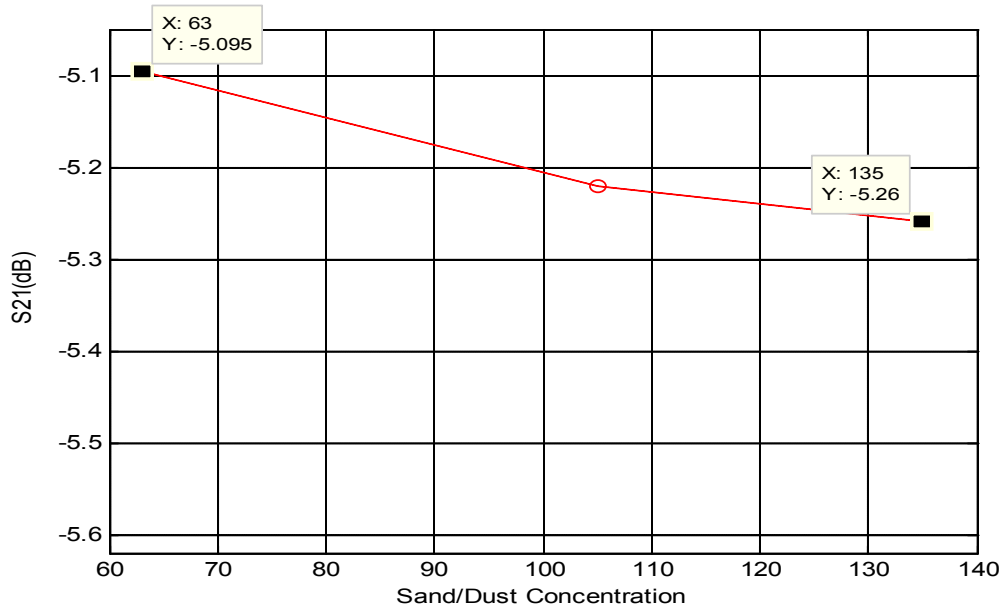


Figure 5.10: S21 response for spherical sand radius of 0.25 cm.

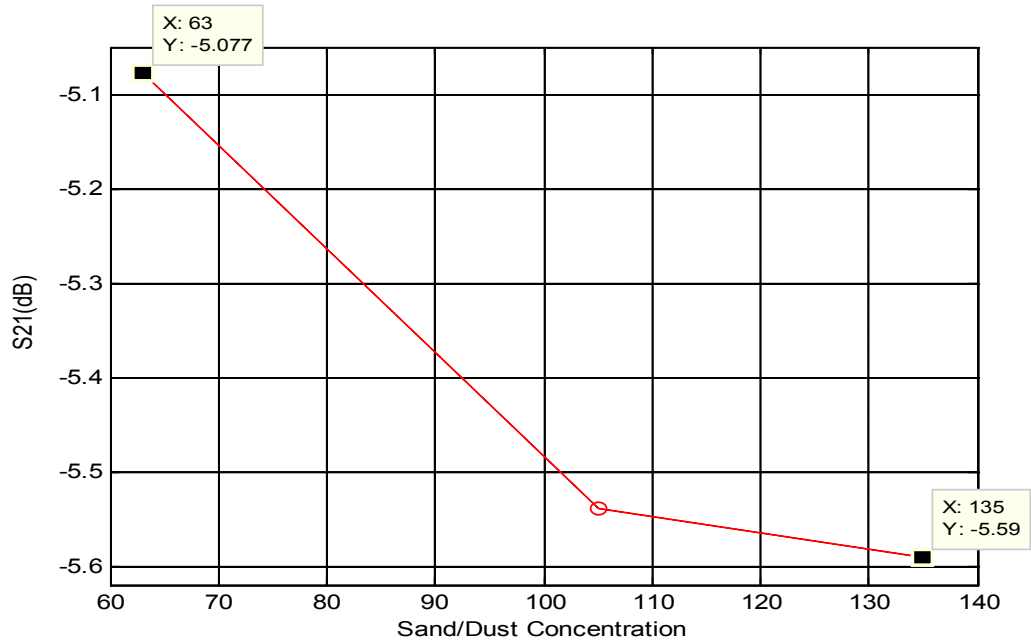


Figure 5.11: S21 response for spherical sand radius of 0.38 cm.

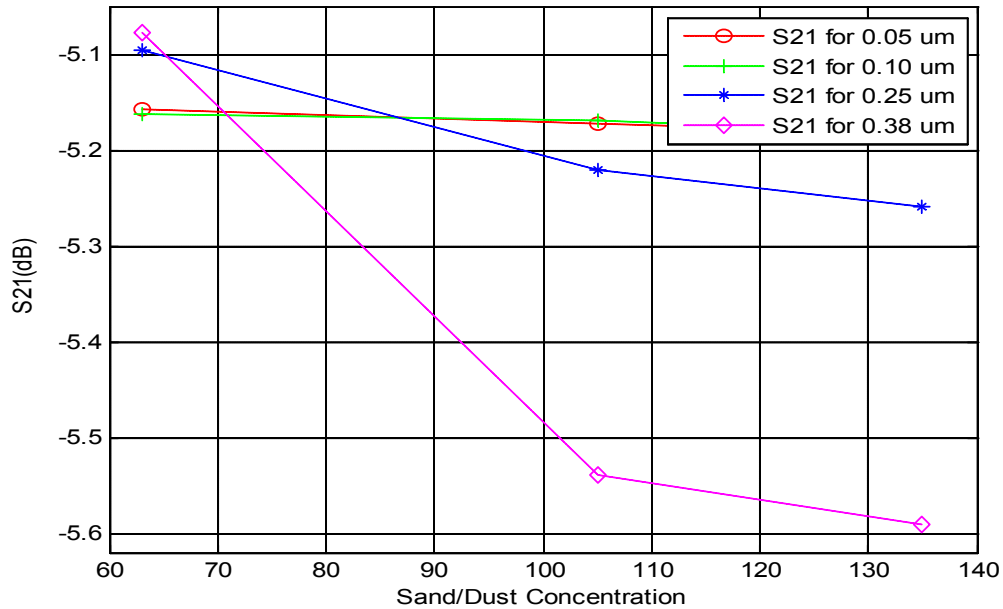


Figure 5.12: Comparison of S21 measurements for variation in sand concentration.

Figure 5.12 shows results from Figure 5.8-Figure 5.11 in a single plot. From here, it is clear that, the difference in the S21 measurements between particle radius  $0.05 \mu\text{m}$  and  $0.10 \mu\text{m}$  is very little. Whereas, attenuation increases a lot when the particle size gets considerably large ( $0.38 \mu\text{m}$ ).

After analyzing all the results for different sand concentrations, it is clear that increasing sand radius increases attenuation, except for the case for 63 balls. Note that the results in Figures 5.8 and 5.9 demonstrated slight reduction of received signals, whereas the responses in Figures 5.10 and 5.11 demonstrate considerable reduction in received signals, particularly for the sand particle concentration of 105 spheres per unit box. The reason behind this may be due to unstable simulation results with smaller sand particles. Further works need to be done with more particles of small sizes like  $0.015 \mu\text{m}$ . Another noteworthy thing is observed that the deviation of concentration from the case of 105

sand spheres to 135sand spheres did not change the transmission response that much. This indicates that after a certain increase in sand concentration, i.e. when the concentration is considerably high, attenuation results do not deviate that much and tend to reach saturation. Even then, the findings of this simulation reiterate that higher density or concentration of sand results in greater transmission losses than that of a lower sand concentration.

## 5.4 Investigation for Elliptical Shaped Sand Particles

After investigating the effects of MW propagation through sand/dust media which consisted of sphere shaped particles, the focus is moved to the elliptical shaped sand particles. Here too, the effects of varying the particle size and sand concentration are tested in a similar manner.

### 5.4.1 For Different Size of Sand Particles

An ellipsoid is a closed quadric surface that is a three dimensional analogue of an ellipse.

Figure 5.13 shows a tri-axial ellipsoid with distinct semi-axes  $a$ ,  $b$  and  $c$ .

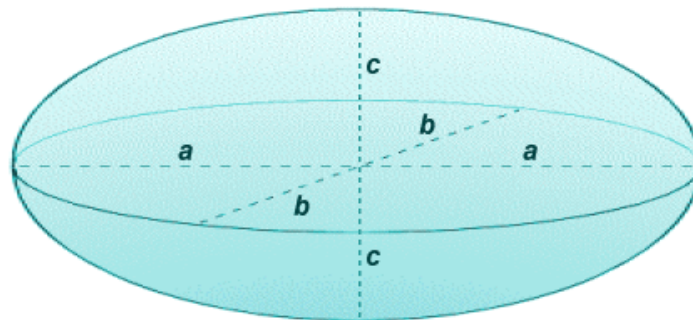


Figure 5.13: A tri-axial ellipsoid.

There are four distinct types of ellipsoids based on the values of  $a$ ,  $b$  and  $c$ . These values represent the length in the  $x$ ,  $y$ , and  $z$  axes, respectively. The particular shape this work chooses to represent as sand particles is one of them. It is known as ‘oblate ellipsoid of revolution’ or ‘oblate spheroid’. For this particular ellipsoid, the values are chosen such that  $a = b > c$ .

For modeling purpose, six sets of values are chosen for investigating the effects on the propagating signal due to the change in sand particle sizes. These sets are:

- I.  $a = b = 0.015$  cm,  $c = 0.012$  cm.
- II.  $a = b = 0.05$  cm,  $c = 0.04$  cm.
- III.  $a = b = 0.010$  cm,  $c = 0.08$  cm.
- IV.  $a = b = 0.25$  cm,  $c = 0.20$  cm.
- V.  $a = b = 0.38$  cm,  $c = 0.30$  cm.
- VI.  $a = b = 0.50$  cm,  $c = 0.40$  cm.

These sets of values are chosen so that the volumes produced by these elliptical sand particles remain in close proximity to the volumes of the spherical sand particles which were chosen previously in this chapter.

There is another important thing to consider about the orientation of the elliptical shaped sand particles inside the box. The oblate spheroid can be placed in two ways, vertical and horizontal. This work tries the both ways to check the effects of change in particle sizes. A comparison can also be made between the vertical orientation and the horizontal orientation of the elliptical sand particles.



Here the transmission responses ( $S_{21}$ ) are observed for one particular sand concentration i.e. 135 sand particles per unit box. The size of the unit box remains the same as mentioned in the previous subsection. The frequency of interest is 9 GHz.

Figure 5.14 shows the transmission responses for 135 elliptical sand particles (vertical orientation) for variation in the sand particle size. The variations in the sizes of the sand particles are done by choosing the six sets of values of  $a$ ,  $b$  and  $c$  which is already mentioned.

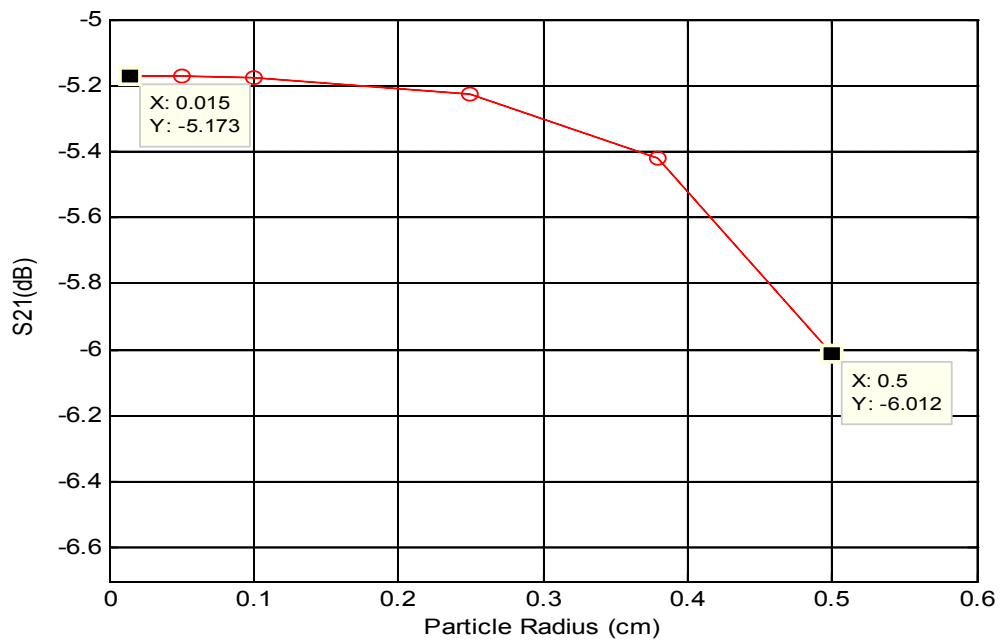


Figure 5.14:  $S_{21}$  response for sand concentration of 135 vertically oriented elliptical sand particles.

It is clear that the transmission loss increases with the increase in particle size.

Figure 5.15 shows the  $S_{21}$  responses for 135 elliptical sand particles which are placed with horizontal orientation.

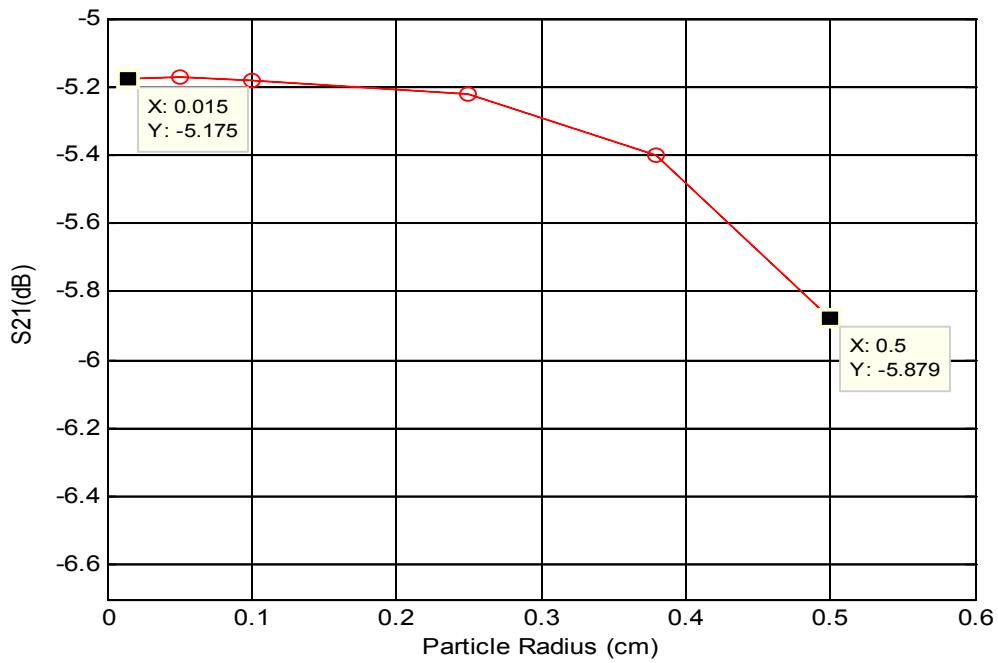


Figure 5.15: S<sub>21</sub> response for sand concentration of 135 horizontally oriented elliptical sand particles.

Like Figure 5.14, here too we find the trend that shows higher transmission losses for bigger sizes of sand particles. While comparing the results for two types of orientation of the elliptical sand particles, except for the largest particles size ( $a=b=0.5$  cm,  $c=0.4$  cm), all the other sizes of particles produce results which are very close to each other.

Figure 5.16 shows a comparison between the S<sub>21</sub> responses for elliptical sand particles with spherical sand particles. The results obtained in Figures 5.14 and 5.15 are superimposed with the results for spherical sand particles with fixed sand concentration of 135 particles (see Figure 5.7).

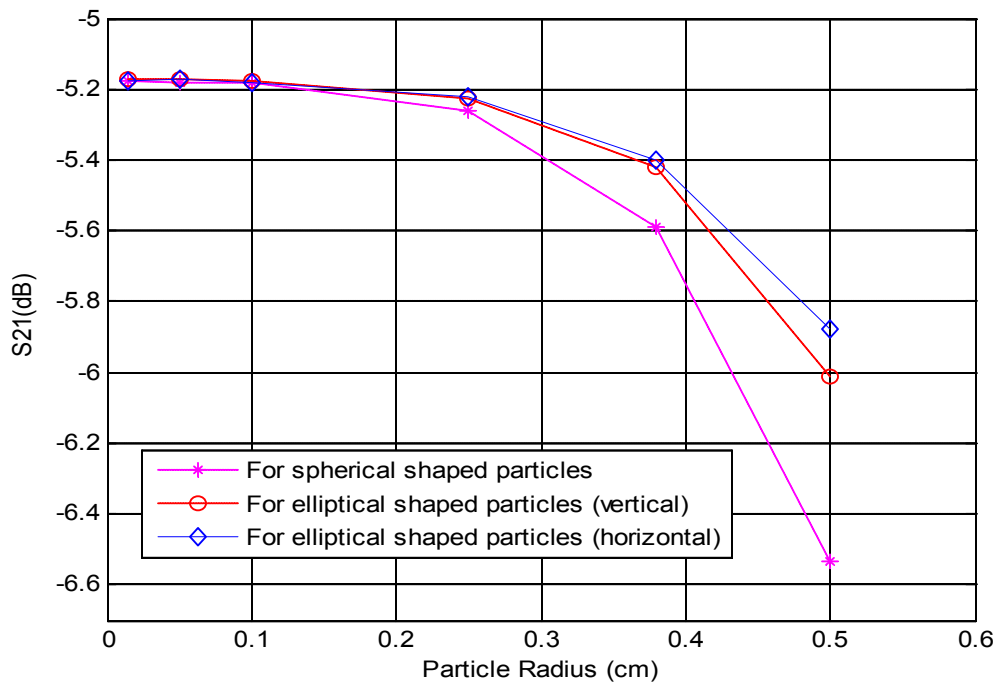


Figure 5.16: Comparison for elliptical shaped sand particles with spherical shaped sand particles, for fixed concentration of 135 sand particles.

From the comparison shown in Figure 5.16, it is clear that the losses for spherical sand particles are higher than that of elliptic particles. It should be noted this deviation is expected as the volumes of the elliptical sand particles actually are 20 % less than the volumes of their corresponding spherical particles.

#### 5.4.2 For Different Concentration of Sand Particles

In subsection 5.3.2, the effects of varying sand concentration was tried for spherical shaped sand particles. Here the same thing is tried for one particular particle size. The chosen size of the sand particle is described by  $a=b=0.25$  cm and  $c=0.20$  cm. Like the case with spherical sand particles, here too, the responses are measured for three different numbers of sand particles, they are: 63, 105 and 135. Figure 5.17 and Figure 5.18 show

the transmission responses ( $S_{21}$ ) for variation in sand concentration for two types of orientations, vertical and horizontal, respectively.

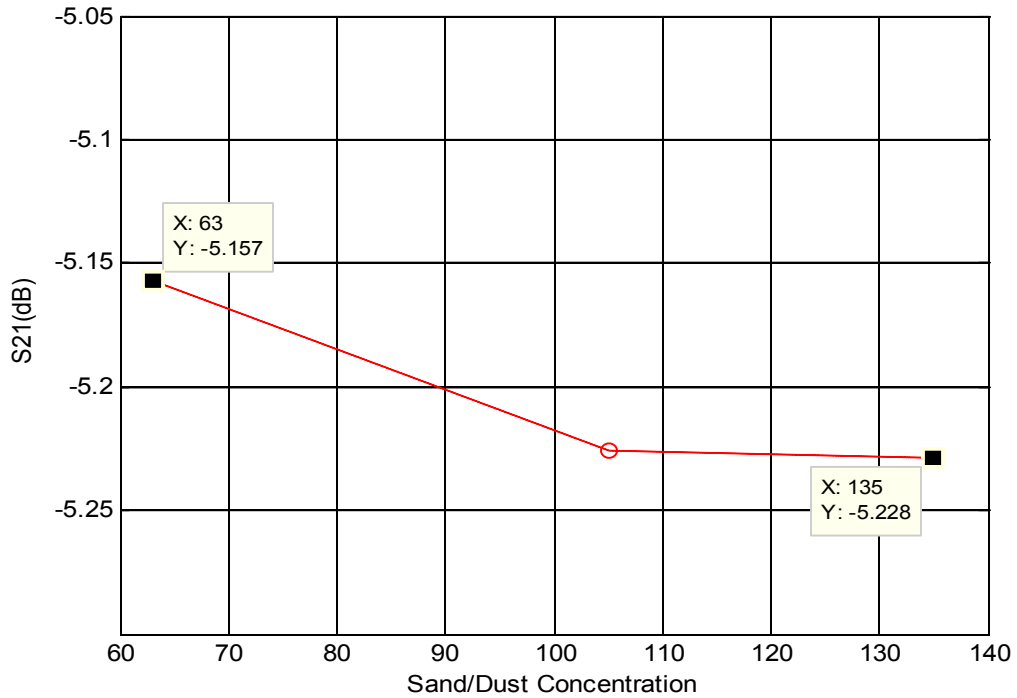


Figure 5.17:  $S_{21}$  responses for elliptical sand particle with  $a=b=0.25$  cm,  $c=0.2$  cm (vertical orientation).

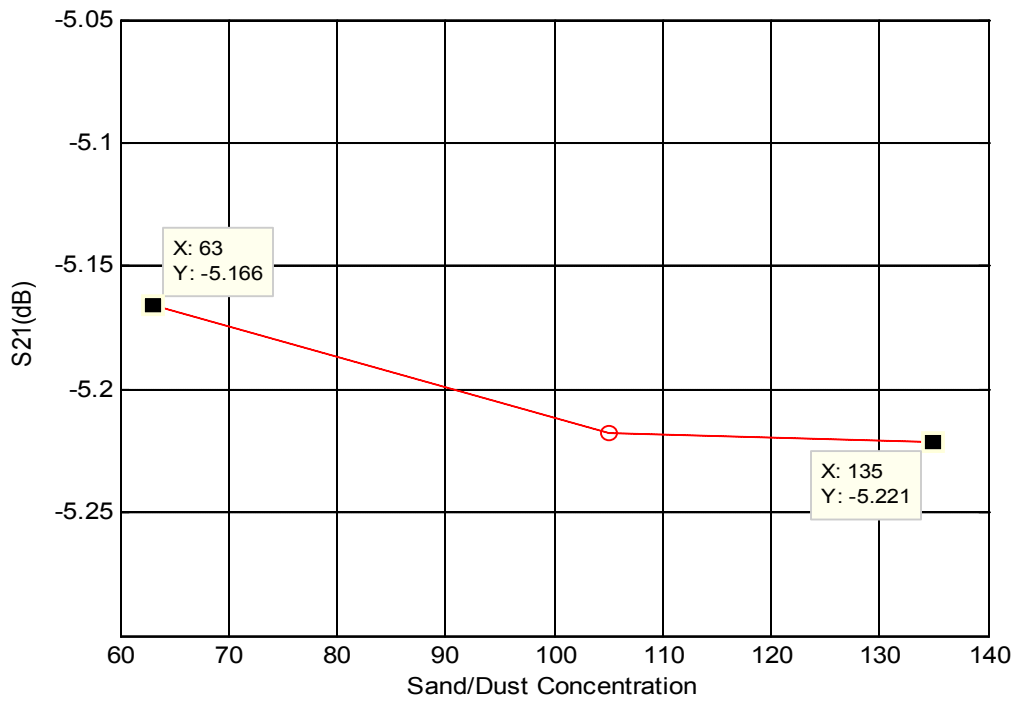


Figure 5.18: S<sub>21</sub> responses for elliptical sand particle with  $a=b=0.25$  cm,  $c=0.2$  cm (horizontal orientation).

From the figures 5.15 and 5.16, it is clear that transmission losses increase with increase in sand concentration. But the responses for 105 sand particles and 135 sand particles are very close to each other.

Figure 5.19 shows a comparison between the S<sub>21</sub> responses for elliptical sand particles with spherical sand particles. The results obtained in Figures 5.16 and 5.17 are superimposed with the results for spherical sand particles with particle radius 0.25 cm (see Figure 5.10).

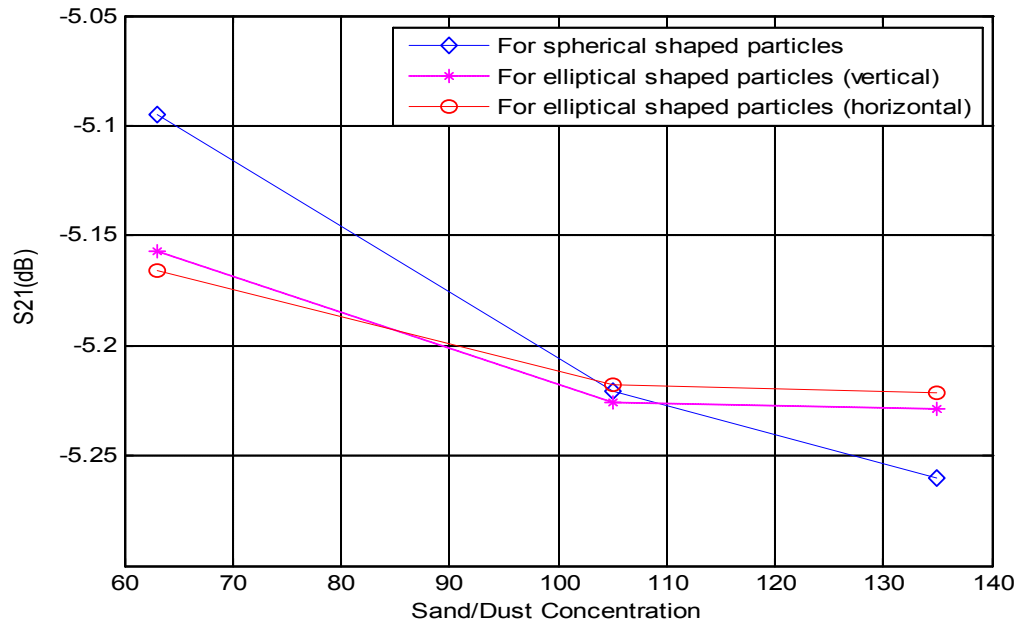


Figure 5.19: Comparison for elliptical shaped particles ( $a=b=0.25$  cm,  $c=0.2$  cm) with spherical shaped sand particles ( $r=0.25$  cm).

The superimposed results in Figure 5.19 indicate that there is very little difference for the two orientations of elliptical particles, though both the orientation deviates much from the results obtained for spherical particles. For low concentration (i.e. 63 sand particles) of sand, spherical sand particles show transmission losses which are lower than that of the elliptical particles. But for high sand concentration (135 particles), the losses for spherical particles are greater than the elliptic particles.

# **CHAPTER 6**

## **COMPARISON OF SIMULATION AND EXPERIMENTAL RESULTS**

### **6.1 Relating Simulation Results to Experimental Observations**

This thesis work aims to investigate the effects of layer based sand/dust media on the propagation of microwave signal. In chapter 4, the disturbances in a microwave link under a sand/dust medium was investigated through a laboratory based experimental setup. In the later part of the same chapter, HFSS software is used to simulate similar experimental setup. Comparing the simulated results with the experimental data, effective permittivity of the mixture of air-sand media was determined. In chapter 5, a modified simulation model was developed to analyze the EM scattering for variation of different parameters of the sand-dust media, such as, particle size, shape and concentration. Due to difficulty in creating a real-size model of the sand-dust storm with acceptable particle concentration, a scaled model was implemented. Using the simulated s-parameter responses, the EM scattering due to variations in the sand-dust particle sizes, shapes and concentration were analyzed.

The results of the simulation model that were presented in chapter 5 were not linked to any real time data for the verification of simulation. Further work has been done in this

chapter to make a comparison between simulated results and the results that were obtained experimentally (which was presented in chapter 4).

### **6.1.1 Design and Analysis of Scaled Simulation Model**

In chapter 4, EM scattering was experimentally investigated using a rectangular box with a width of 60 cm, length of 80 cm and height of 60 cm. The air-sand dielectric material within the box was enclosed by a 4 mm thick plastic wall with air-inlet valves. The rectangular horn antennas attached to both side of the air-sand box were used to excite and receive an X-band frequency sweep. The box was filled with air-sand mixture for sand particle sizes of 90  $\mu\text{m}$ , 125  $\mu\text{m}$  and 150  $\mu\text{m}$ . The concentration of the air-sand mixture was controlled by putting a particular volume of sand particles within the air-box. To better match the experimental data with simulated results, the modified simulation model of chapter 4 investigated EM scattering due to change in different particle shape, size and concentration. In this chapter, one particular approach is tried to scale the simulation scenario to match up with the experimental setup.

For the experimental results, the transmission response for the sand sample of diameter 150  $\mu\text{m}$  is considered. And for the simulation results, the transmission response for the case of 135 spherical particles with particle diameter 1000  $\mu\text{m}$  is considered. The particle used in simulation is about 6.67 times bigger that the particles used in experimental. Thus 6.67 is chosen as the scaling parameter. As the objective is to match the experimentally obtained  $S_{21}$  responses for sand diameter of 150 $\mu\text{m}$ , the frequency of interest for simulation is chosen as (9 GHz  $\div$  6.67) or 1.35 GHz. Thus, this scaling maintained the same ratio of the simulated wavelength to particle size to that of the experimental setup.



But the operating frequency 1.35 GHz required a horn antenna larger than the dimension of the propagation box. So a slightly adjusted frequency of 1.5 GHz is adopted to reduce the horn antenna size to match up to the dimensions of 12 cm width and 12 cm height.

To match the ratio of wavelength of the signal to the length of the simulation box, an equivalent box in the experimental setup would have dimensions which are 6.67 times less than the dimensions of the simulation box. Thus, the dimensions of the box in the scaled-up simulated model with dimensions of 12 cm x 20 cm x 12 cm, corresponds to a small rectangular section of the experimental box (of chapter 4) with dimensions of 1.8 cm x 3 cm x 1.8 cm.

The scaled-up version of the modified simulated model is shown as Box A in Figure 6.1. The corresponding rectangular section within the experimental box of chapter 4 is shown as Box B in Figure 6.1. Thus, the EM scattering (specifically attenuation) of Box A should correspond to Box B due to equal scaling of all parameters including box-size, sand-particle size, operating frequency etc. So EM attenuation obtained from the simulated S-parameters of this model can be directly compared with experimentally observed results.

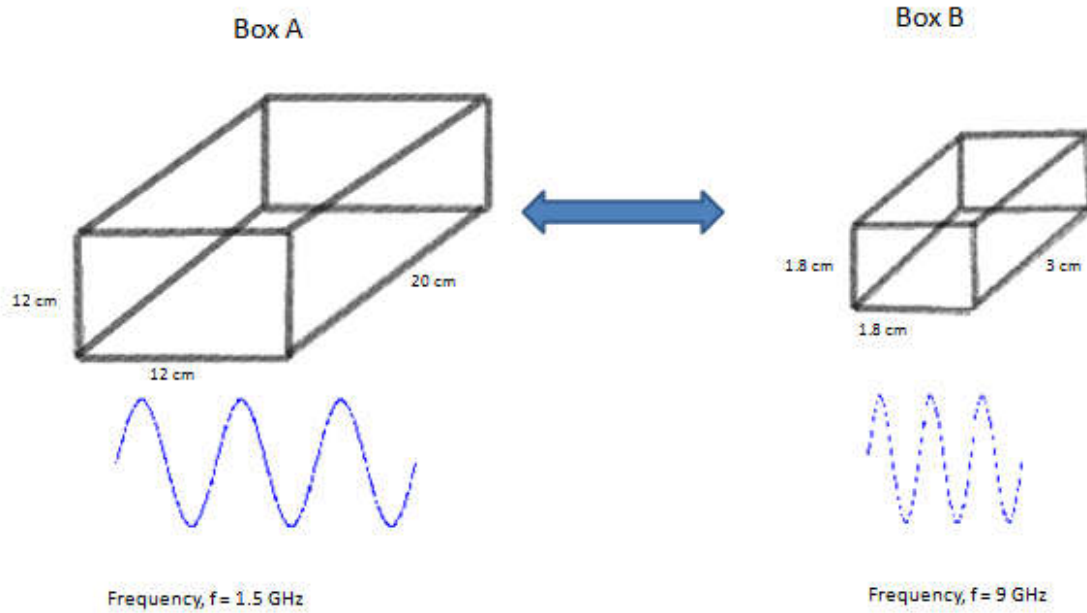


Figure 6.1: Simulated responses for Box A at 1.5 GHz are equivalent to the experimental responses for Box B at 9 GHz.

The simulated S-parameter ( $S_{21}$ ) response of Box A, containing 135 randomly distributed spherical sand particles with diameter of 0.1 cm is shown in Figure 6.2. For comparing this result with the  $S_{21}$  obtained without sand particles i.e. the results for box containing only air is also superimposed in this figure.

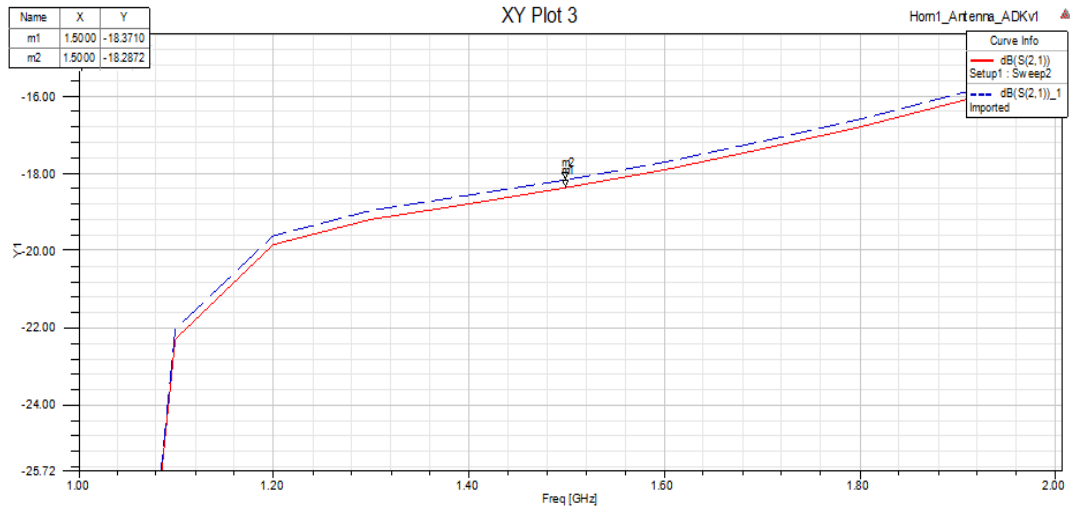


Figure 6.2: Comparison of  $S_{21}$  responses of Air-Sand and Air-only cases(Box A).

Note that the transmission response of propagating EM signal improves with increasing frequency. But due to the selected scaling factor, the attenuation due to air-sand dielectric media at 1.5 GHz remained important. The measured and simulated responses are calibrated by subtracting the  $S_{21}$  values of the air-sand mixture from that of air-only case. This allowed us to record the losses of the propagating EM wave due to sand particles only. The observed attenuation for selected sand sample demonstrated by the scaled-up simulated model (Box A), which is tabulated in Table 6.1, corresponds to losses of a smaller rectangular section (Box B of Figure 6.1) of the experimental setup presented in chapter 4.

Table 6.1: Simulated and Experimental  $S_{21}$  responses with their corresponding losses.

	Simulated results at 1.5- GHz for box with dimensions of 12 cm x 12 cm x 20 cm	Experimental results at 9- GHz for box with dimensions of 60 cm x 60 cm x 80 cm
$S_{21}$ for Air Only (dB)	-18.287 dB	-18.75 dB
$S_{21}$ for Air-Sand Mixture (dB)	-18.371 dB	-23.3 dB

Using the linear power-ratio scale and assuming uniform attenuation, the extrapolated attenuation of the whole experimental box can be calculated and found as 0.027 dB/80 cm. This value is presented in Table 6.2 along with the attenuation which is calculated from the experimentally observed measurement of  $S_{21}$  responses.

Table 6.2: Attenuation due to sand particles for an 80 cm link.

	Simulated results 9 GHz (extrapolated from 1.5 GHz response)	Experimental results at 9 GHz
Attenuation due to Sand particles (dB/80cm)	0.027 dB/80cm	0.0376 dB/80cm

The difference in experimental and simulated attenuations is quite low and could be attributed to the error in assumption of the sand particle distribution, difference in shape, concentration, presence of the moisture content in sand particles etc.

### 6.1.2 Comparison of Attenuation with Values Obtained from Literature

In Table 6.2, it is shown that the calculated attenuations for an 80 cm link due to the presence of sand particles are 0.0376 dB (experimental results) and 0.027 dB (simulation results). The measured S21 values are converted to linear scale before subtracting the air-sand values from air-only case. This manual calibration allowed us to monitor the attenuation due to sand-particles of the propagation box. For comparison with the literature, the attenuation due to 1m link is extrapolated from that of 80 cm. Thus, the attenuations are calculated as 0.047 dB/m (experimental results) and 0.034 dB/m (simulation results). These values are comparable to the measured attenuation of Haddad et al. [21], which is 0.034 dB/m at the frequency of 9.4 GHz. But their measured attenuation is 30 times larger than their calculated attenuation of 0.001 dB/m [21]. This problem was unexplained until 2005, when Zhou et al. [37] and He et al. [38] included the effect of charges carried by the sand particles. Their work showed that the attenuation coefficients for charged sand particles could be as high as the measured results reported by Haddad et al. [21]. Thus, the difference between the attenuation measured experimentally and obtained through calculation of Haddad's work gets resolved when the effects of charged sand particles are considered. Li et al. [39] calculated attenuation for partially charged sand particles. For a given charge to mass ratio of  $-10 \mu\text{C}/\text{kg}$ , this attenuation can be approximated as 0.05 dB/m at 9 GHz [39]. Table 6.3 tabulates the different attenuation values for 1 m link for the purpose of comparison.

Table 6.3: Comparison of the different Attenuation values(dB/m).

Attenuation obtained from optimized simulator model (at 9 GHz)	Attenuation calculated from experimental results (at 9 GHz)	Attenuation obtained from the work of Haddad et al. [21] (at 9.4 GHz)	Attenuation Obtained from the work of Li et al. [39] (at 9 GHz)
0.034 (dB/m)	0.047 (dB/m)	0.034 (dB/m)	0.05 (dB/m)

## 6.2 Investigation of Effects of Polarization through Simulation

Polarization is an important property of propagating electromagnetic wave, as discussed in Chapter 3. It mostly describes the orientation of the electric field (E-field) component of the propagating EM wave. Typically, linearly polarized EM waves are either vertically or horizontally polarized, and the orientation of the rectangular horn antenna with horizontally or vertically directed E-field are used to excite or receive them. Thus, in the simulation model, the polarization effects of the propagating EM wave due to air-sand/dust media can be observed by rotating the orientation of the receiver horn antenna from vertical to horizontal direction. This allowed the reception of the horizontally polarized waves exiting the propagating area. This method is used here for the air-sand filled scaled simulation model with box dimensions of 12 cm x 12 cm x 20 cm. The simulations are performed for elliptical sand particles too with vertical and horizontal orientation (as explained in chapter 5). Three measurements are taken to make the comparison which involves both the particle shapes this study has approached so far, spherical and elliptical. At first, 135 spherical sand particles are considered for a particle

radius of 0.05 cm. The second case considers 135 vertically oriented elliptical particles with size  $a = b = 0.05$  cm and  $c = 0.04$  cm. Finally 135 horizontally oriented elliptical particles with same values of  $a$ ,  $b$  and  $c$  are considered.

Comparing the transmission responses of the vertically and horizontally polarized received signals of all these cases, the effects on the polarization of the propagating EM wave is predicted. The transmission responses for two types of polarizations for spherical shaped sand as well as vertically and horizontally oriented elliptical shaped sand are given in Table 6.4.

Table 6.4: Simulated  $S_{21}$  values for different polarizations and different shapes of sand particles.

	Spherical Sand Particles	Vertically Oriented Elliptical Sand Particles	Horizontally Oriented Elliptical Sand Particles
S21 for Vertical Polarization (dB)	-18.3710	-18.3611	-18.3661
S21 for Horizontal Polarization (dB)	-18.3727	-18.3851	-18.375

From the results shown in Table 6.4 it is clear that there are certain deviations in the  $S_{21}$  measurements for two different polarizations of electric field. To determine the effect of this polarization, results for horizontal polarization for spherical sand particles is used to calculate the losses for the presence of sand particles and it is found to be 0.029dB/80 cm. As mentioned in the section 6.1 this loss was calculated to be 0.027 dB/80 cm (vertical

polarization). According to these results, it is clear that the differences due to change in polarization could have a greater impact when the losses are calculated for a larger link.



## CHAPTER 7

### SUMMARY AND CONCLUSION

This research work investigated the effects of a microwave signal propagating through sandy/dusty medium. Initially these effects were observed by monitoring the transmission responses of a laboratory setup made of a non-guided propagation box. Properly aligned horn antennas were used as transmitter and receiver. Attenuations due to sand particles within the propagation box were calculated by subtracting the transmission responses of air-sand mixture from that of the air-only case. Then using the professional simulator software (HFSS), a modified simulation setup was modeled to monitor S-parameter responses. By comparing the experimental and simulated results, the simulator model was fine tuned in terms of excitation and mesh size etc. The validated simulator model was then used to investigate the effects of parameters like sand particle concentrations, shapes and sizes etc. The polarization effects on EM scattering were also investigated by using the same model. The overall summary, conclusion and future prospects of the work are presented in the following sections.

#### 7.1 Summary

- A thorough literature survey on the attenuation of the propagating microwave signal due to suspended particles of sand-storm was presented.

- In the literature, layer based sand storm was defined as smaller sand particles reside in the upper layer. But EM scattering due to different layers of sand storm containing different sized sand particles was absent in the literature.
- Using the Sieve Analysis, different sized sand particles were collected. The three collected sand samples consisted of particles with diameters of: 90  $\mu\text{m}$ , 125  $\mu\text{m}$  and 150  $\mu\text{m}$ .
- A series of transmission response measurements ( $S_{21}$ ) for a rectangular waveguide filled with air-sand mixture were performed for three sand samples. Blowers installed using non-radiating slots were used to distribute the sand particles to resemble sand-storm. A vector analyzer was used to record the responses and attenuation due to sand samples was calculated. The  $S_{21}$  results were used to validate a simulation model of a similar set-up which was constructed by using the professional EM simulator (HFSS). The simulator was used to back calculate the effective dielectric constants of three different uniform air-sand mixtures.
- A similar non-guided propagation set-up was created in the laboratory. This included a plastic box with optimally positioned air blowers and air-only valves. Aligned transmitting and receiving horns were placed at both ends of the box and were connected to a network analyzer.
- $S_{21}$  responses were measured for all the three sand samples with known concentration and related attenuation due to sand samples was calculated.
- A simulator model was developed for the investigation of the non-guided propagation of microwave signal through the plastic box, filled with uniform air-sand media of certain effective permittivity. The experimental S-parameters were

used as a reference and effective permittivity values were varied until simulated S-parameters gave same/similar values.

- But the shortcoming of this approach was that the software model ignored the influences of sand/dust particle shapes, sizes and concentrations, which may have produced changes in polarization, S-parameters etc.
- After that, a modified simulation model was tried where sand particles of different sizes, shapes, and concentrations were included to investigate how attenuation and polarization of the propagating X-band microwave signal gets affected due to individual parameters of the layered sand-storm.
- Attenuation due to sand samples observed from the modified scaled simulator model and the experimental setup were compared for an arbitrarily selected frequency of 9 GHz. This validated the simulated model for non-guided propagation.
- While comparing results for different sand concentrations, it was found that higher density of sand particles lead to a higher loss.
- The results of this simulation model were then scaled and superimposed to match the scenarios which were exploited earlier through experimental findings. A comparison was drawn between the experimental findings and the results obtained from the simulation model.
- To observe the polarization changes due to particle shape and orientation, spherical and elliptical particles were included in the simulated model. The E and H plane microwave signals, received by the horn antenna, were recorded and analyzed.

## 7.2 Conclusion

The Middle East is one of the regions which experience severe sand/dust storm throughout different times in a year. The reliability and stability of the wireless communication links get affected during these times and to ensure the quality of service, a proper way of understanding and analyzing of these events is required.

This work aims to investigate the transmission responses of microwave signals under sandy/dusty media. At first, the effects were observed experimentally by using three different sand sample of diameter  $90\ \mu\text{m}$ ,  $125\ \mu\text{m}$ , and,  $150\ \mu\text{m}$ . Later these findings were tried to be matched through different simulation approaches. This was done in the pursuit of a simulation model that can take account of different parameters which are associated with the propagation of microwave signal under such conditions. Finally a simulation model was introduced which is convenient for tackling issues concerning different particle radii, frequencies, variations in sand concentration, polarizations etc. All the findings of the simulation models reiterate the finding that for different sand particle size, different attenuations are experienced. And a heavier sand concentration leads to a greater loss in signal transmission responses. Using this model can be proven to be useful in predicting signal attenuation under different circumstances related to Sandy/Dusty weather.

Later the simulation model was modified and scaled in order to make a comparison of the attenuation obtained from the experimental results. For a link of 1 m, attenuation was calculated as 0.047 dB from experimental results. The corresponding simulated

attenuation was calculated as 0.034 dB/m. Finally these values were compared with the values obtained from the literature and they agreed well.

There have been some limitations as well in the approaches taken in this study. The experimental data that were recorded manually using a vector analyzer, has some instrumental errors. Again, in the simulation model that used spherical and elliptical shapes to represent sand particles, the total number of particles was limited. It was quite difficult to put a large number of sand spheres manually in order to keep the distribution random.

### **7.3 Future Works**

- The experimental measurements could be taken outside the laboratory and a greater range for exploitation of signal in terms of distance could be tested.
- While this work contained study of MW signals in X band frequency, frequencies in other bands could also be used in the measurements.
- Another important aspect could be to quantify visibility with sand concentration as visibility is such a key parameter in the study of signal attenuation. A simulation model could be a pursuit to establish the relation.
- The proposed simulation model could be tested for more combinations at different geometric test scenarios.
- The effect of polarization could be tested more accurately by putting a larger number of sand spheres inside the box.

## References

- [1] ANSARI, A.J., and EVANS, B.G. : 'Microwave propagation in sand and dust storms', IEE Proc. F, Commun., Radar & Signal Process. 1982, 129, pp.315-322.
- [2] Article on Daily Mail on the date of January 11, 2013, Available at: <http://www.dailymail.co.uk/news/article-2260560/Wall-sand-whipped-Tropical-Cyclone-Narelle-hits-Onslow-Western-Australia.html>].
- [3] Dong, X.Y., Chen, H.Y., Guo, D.H., 'Microwave and Millimeter-Wave attenuation in sand and dust storms', IEEE ANTENNAS AND WIRELESS PROPAGATION LETTERS, VOL. 10, 2013.
- [4] J. Goldhirsh, "Attenuation and backscatter from a derived two-dimensional duststorm model,"IEEE Trans. Antennas Propagat., vol. 49, no. 12, pp. 1703–1713, Dec. 2001.
- [5] T. S. Chu, "Effect of sand storms on microwave propagation," Bell Syst. Tech.J., vol. 58, pp. 549–555, 1979.
- [6] Zain Elabdin, Md.Rafiqul Islam" Dust storm Measurements for the Prediction of Attenuation on Microwave Signals in Sudan", International Conference on Computer and Communication Engineering 2008 (ICCCE'08) Kuala Lumpur, May 2008.

- [7] Kamal Harb, Omair Butt, Samir Abdul-Jauwad, Abdullah Al-Yami, A-Yami, “A Proposed Method for Dust and Sand Storms Effect on Satellite Communication Networks”.
- [8] Sami M. Sharif, “Dust Storms Properties Related to Microwave Signal Propagation”, UofKEJ Vol. 1 Issue 1 pp. 1-9 (June 2013).
- [9] Abuhdima, E. M., I. M. Aleh, “Effect of sand and dust storms on microwave propagation signals in Southern Libya”, *2010 15<sup>th</sup> IEEE Mediterranean Electrotechnical Conference*, 695-698, 2010.
- [10] Elabdin Z., M. R. Islam, O. O. Khalifa, and H. E. A. Raouf, “Mathematical model for the prediction of microwave signal attenuation due to dust storm”, *Progress In Electromagnetics Research M*, Vol. 6, 139-153, 2009.
- [11] Qun-feng Dong, Ying-Le Li, Jia-dong Xu, Hui Zhang, Ming-jun Wang, “Effect of Sand and Dust Storms on Microwave Propagation”, *IEEE Transactions On Antennas and Propagation*, Vol. 61, No.2, February 2013.
- [12] S. Ahmed, A. Ali, and M. A. Alhaider, “Airborne dust size analysis for tropospheric propagation of millimetric waves into dust storms,” *IEEE Trans. Geosci. Remote Sens.*, vol. 25, no. 5, pp. 593–599, Sep, 1987.
- [13] A.S. Ahmed, “Role of particle-size distributions on millimeter-wave propagation in sand/duststorms,”*Inst. Electr. Eng.Proceedings*, vol. 134, pp. 55–59, 1987.
- [14] Elfatih A. A. Elsheikh, Md. Rafiqul Islam, Al-Khateeb, AHM Zahirul Alam, Zain O. Elshaikh,” A Proposed Vertical Path Adjustment Factor for Dust Storm

Attenuation Prediction'', 4th International Conference on Mechatronics (ICOM), Kuala Lumpur, Malaysia, May, 2013.

- [15] AL-HAFID, H.T., GUPTA, S.C., and BUNI, K. : 'Effect of adverse sand storm media on microwave propagation', Proc. National Radio Science Meeting, URSI.8, 1979, p.256.
- [16] RYDE, J.W. : 'Echo intensities and attenuation due to clouds, rain, hail, sand and dust storm at centimeter wavelengths', Report 7831, Research Laboratories of General Electric Company Ltd., 1941, pp. 22-24.
- [17] AHMED, I.Y. : ' Microwave propagation through sand and dust storms', PhD Thesis, University of Newcastle Upon Tyne, UK, 1976.
- [18] Louza, S. , N. F. Audeh, "Effect of dust on microwave radiometry", *1992 IEEE Aerospace Applications Conference, Digest*, 107-136, 1992.
- [19] Renno, N. O., A. S. Wong, S. K. Atreya, "Electrical discharges in the martian dust devils and dust storms", Sixth International Conference on Mars, Pasadena, California, 2003.
- [20] GHOBRIAL, S.I., ALI, I.A., and HUSSEIN, H.M. : 'Microwave attenuation in sand storms', Proc. Int. Symp. Antenna and Propagation, Sendai, Japan, 1978, pp.447-450.
- [21] HADDAD, S., SALMAN, M.J.H., and JHA, R.K.: 'Effect of dust/ sand storms on some aspects of microwave propagation', *ibid.*, pp. 153-161.



- [22] RAFUSE, R.P.: 'Effectsofsandstormsandexplosion generated atmospheric dust on radio propagation', MIT, Lincoln Lab, Lexington, 1981, Project Report DCA-16, ESD-TR-81-290.
- [23] AL BADER, S.J., and DAWOUD, M.M. : 'Measurements of the complex refractive index of soils and airborne particles', Proc. URSI Commission FSymposium, Louvain-la-Neuve, Belgium, 1983, ESA publication SP-194, pp.149-152.
- [24] GHOBRIAL, S.I.: 'Effect of hygroscopic water on dielectric constant of dust at X-band', Electron. Lett., 1980, 16, pp, 393-394.
- [25] SHARIEF, S.M., and GHOBRIAL, S.I. : 'X-band measurements of the dielectric constant of dust', Proc. URSI Commission FSymposium, Louvain-la-Neuve, Belgium, 1983, ESA publication SP-194, pp. 143-14.
- [26] GOLDHIRSH, J. : 'A parameter review and assessment of attenuation and backscatter properties associated with dust storms over desert regions in the frequency range of 1 to 10 GHz', IEEE Trans., 1982, AP-30, pp. 1321-1329.
- [27] [http://www.ie.itcr.ac.cr/acotoc/Maestria\\_en\\_Computacion/Sistemas\\_de\\_Comunicacion\\_II/Material/Biblio1/chapter%2010.pdf](http://www.ie.itcr.ac.cr/acotoc/Maestria_en_Computacion/Sistemas_de_Comunicacion_II/Material/Biblio1/chapter%2010.pdf).
- [28] David Pozar, "Microwave Engineering", Willey and sons, 2005.
- [29] Gobrial, S. I., "The effect of sand storms on microwave propagation", Proc. Nat. Telecommunication Conf., Vol. 2, 43.5-43.5.4, Houston, Texas, 1980.
- [30] Sharif, S., "Performance of earth-satellite links during dust storms at the X-band", Sudanese Engineering Journal, Vol. 40, No. 33, 1993.

- [31] Soil Properties and Qualities-Natural Resources Conservation Service, Available online at:  
[http://www.nrcs.usda.gov/wps/portal/nrcs/detail/soils/ref?cid=nrcs142p2\\_054224](http://www.nrcs.usda.gov/wps/portal/nrcs/detail/soils/ref?cid=nrcs142p2_054224).
- [32] The COMET Program, “Atmospheric Dust Module”, Available online at:  
<http://www.meted.ucar.edu/atdust/>.
- [33] Von Hippel A. R. et al., “Table of Dielectric materials,” Lab Insul. Res., M.I.T., Cambridge, MA, Tech. Rep. 57, Vol IV, Jan. 1953.
- [34] A. Arun and T. K. Sreeja, “An effective downlink budget for 2.24 GHz-S Band LEO Satellites”, *IEEE Conference on Information Communication Technologies (ICT)*, 2013, pp. 342-345.
- [35] K. Harb, S. Abdillah, and S. Abdul-Jauwad, “Dust and Sand (DUSA) storms impact on LEO satellite microwave radio links,” *Advanced Satellite Multimedia Systems Conference and the 13<sup>th</sup> Signal Processing for Space Communications Workshop (ASMS/SPSC)*, 2014, pp. 442-447.
- [36] M. Hamidi, M.R. Kavianpour, and Y. Shao, “Synoptic analysis of dust storms in the Middle East,” *Asia-Pac. J. Atmospheric Sci.*, vol. 49, no.3, 2013, pp. 279-286.
- [37] Y. Zhou, Q. He, and X. Zheng, “Attenuation of electromagnetic wave propagation in sandstorms incorporating charged sand particles,” *Eur. Phys. J. E* 181-187 (2005).

- [38] Q. S. He, Y. H. Zhou and X. J. Zheng, "Effects of charged sand on electromagnetic wave propagation and its scattering field," *Sci. China Ser. G Phys. Mech. Astron.* 49, 77-87 (2006).
- [39] X. Li, L. Xingcai and Z. Xiaojing, "Attenuation of an electromagnetic wave by charged dust particles in a sandstorm," *6756 Applied Optics*, Vol. 49, No. 35.

# Vitae

- Name: Mahfuz Ullah
- Nationality: Bangladeshi
- Date of Birth: 27 March, 1988
- Email: mahfuz.kfupm@gmail.com
- Permanent Address: Viilage: Dignagar, Post: Benipur,  
Police Station: Shailokupa, Upazila: Shailokupa,  
Zilla: Jhenaidah, Bangladesh
- Academic Background:
  - Master of Science (M.S.) in Electrical Engineering, Department of EE, King Fahd University of Petroleum and Minerals, December, 2015.
  - Bachelor of Science (BSc.) in Electrical and Electronic Engineering, Department of EEE, United International University, Dhaka, Bangladesh, January, 2011.
- Publication:
  - Ullah, M., Iqbal, S. S. (2015). Effects of Sand Particle Radius on Attenuation of Microwave Signal Under Sand & Dust Storm. – Manuscript ready for publication-Journal, December, 2015.
  - Ullah, M., Iqbal, S. S. (2015). Simulation Based Analysis of Microwave Signal Propagation Under Sand/Dust storm . – Manuscript ready for publication- Conference Proceedings, December, 2015. |